Seasonal monitoring of lipid degradation processes in the western English Channel links bacterial 10S-DOX enzyme activity to free fatty acid production by phytoplankton

Jean-Francois Rontani, Lukas Smik, Frédéric Vaultier, Claire Widdicombe, Simon Belt

Seasonal monitoring of lipid degradation processes in the western English Channel links bacterial 10*S*-DOX enzyme activity to free fatty acid production by phytoplankton

Jean-François Rontani[1*], Lukas Smik[2], Frédéric Vaultier[1], Claire Widdicombe[3], Simon T. Belt[2]

[1] Aix Marseille Univ, Université de Toulon, CNRS, IRD, MIO UM 110, Marseille, France, 13288, Marseille, France.

[2] Biogeochemistry Research Centre, School of Geography, Earth and Environmental Sciences, University of Plymouth, Drake Circus, Plymouth, Devon PL4 8AA, UK.

[3] Plymouth Marine Laboratory, Prospect Place, West Hoe, Plymouth PL1 3DH, UK

* Corresponding author. Tel.: +33-4-86-09-06-02; fax: +33-4-91-82-96-41. E-mail address: jean-francois.rontani@mio.osupytheas.fr (J.-F. Rontani).

Abstract. In a few recent studies, the action of a bacterial dioxygenase (10*S*-DOX) on palmitoleic acid was observed within some polar and estuarine settings. To add further mechanistic information regarding the action of this enzyme in marine settings, we measured a range of lipids (sterols, fatty acids and the chlorophyll phytyl side chain) and their biotic and abiotic degradation products in water samples collected in 2018 from two depths (5 m and 25 m) at the temperate oceanographic time series site L4, located in the western English Channel. Lipid distributions indicated a dominance of diatoms and copepods during the spring bloom, while a peak in dinoflagellate activity was evident in samples collected from late summer/autumn, both outcomes being consistent with taxonomic data reported previously for the same sampling site and interval. Monitoring of lipid oxidation products characteristic of different degradation pathways showed a relatively weak effect of photo- and autoxidation processes, with these acting mainly on the more reactive lipids (i.e. chlorophyll and polyunsaturated fatty acids). In contrast, monitoring of biotic degradation processes revealed significant quantities of 10*S*-hydroxyhexadec-8(*E*)-enoic acid in samples collected at the end of April (reaching 40% of the residual parent palmitoleic acid), attributed to the involvement of bacterial 10-dioxygenase (10*S*-DOX) activity during the spring bloom. We propose that this enzyme could be utilised by bacteria to detoxify free fatty acids released by wounded diatoms in the presence of copepods

Keywords: Biotic and abiotic degradation; 10S-DOX enzymatic activity; Bacteria; Wounded diatoms.

1. Introduction

Suspended particles sink very slowly through the water column and constitute most of the standing stock of particulate matter in the oceans (Bacon et al., 1985; Wakeham and Lee, 1989). These particles are composed of a heterogeneous mixture of biogenic, lithogenic, and authigenic components, with their relative proportions dependent on location and depth. However, biogenic (mainly phytoplanktonic) material normally dominates particle composition in the upper 100 m (Honjo et al., 1982). Suspended particles are also generally considered to contain more highly degraded organic matter (OM) than sinking particles due to their longer residence times in the water column (Tanoue and Handa 1980). However, several previous field-based studies have shown high abundances of relatively undegraded labile material in suspended particles (Lee et al., 1983; Wakeham et al., 1985; Wakeham and Canuel, 1988; Sheridan et al., 2002). It is thus important to understand: (i) the mechanisms by which such organic matter is degraded in the water column, and (ii) the relative importance of biotic vs. abiotic processes responsible for this degradation.

Biotic degradation of algal material in the water column depends not only on zooplankton grazing (Harvey et al., 1987), but also on the remineralization activity of the associated bacteria. Indeed, particles are rapidly colonized by prokaryotes, and particle-attached communities are often more metabolically active (Grossart et al., 2003; 2007) and phylogenetically diverse (Ortega-Retueta et al., 2013; Ganesh et al., 2014) than free-living assemblages.

Although less widely studied than its biologically mediated (heterotrophic) counterpart, abiotic degradation by processes such as photooxidation and autoxidation (spontaneous free radical reaction of organic compounds with oxygen) is now understood to play a role in the fate of phytoplankton in the ocean (for a recent review, see Rontani and Belt, 2020). While, due to the presence of chlorophyll *a*, a very efficient photosensitizer (Foote, 1976), visible-light-induced photosensitization involves mainly reaction with singlet oxygen ($^1O_2$) and acts on the

unsaturated lipid components of algae, the mechanism by which autoxidation is initiated in phytodetritus appears to be homolytic cleavage of photochemically-produced hydroperoxides (Girotti, 1998; Rontani et al., 2003). Consequently, both photooxidation and autoxidation can significantly affect the composition of lipids in suspended particles (Rontani and Belt, 2020).

Lipids, which constitute one of the three main classes of organic matter in algal material (Sun et al., 2002), are less labile than carbohydrates and proteins and are thus often used as biomarkers to determine the sources (Volkman, 1986, 2003) and the alteration state of specific organisms (Rontani et al, 2012; 2016).

In the present work, we monitored the biotic and abiotic degradation of lipids in suspended particle material (SPM) collected in 2018 from the Western Channel Observatory (WCO, https://www.westernchannelobservatory.org.uk/) marine station L4, which is a highly seasonal temperate shelf site (Widdicombe et al 2010, Atkinson et al 2015, Cornwell et al 2020). A focus of the study was the action of a particular bacterial enzyme (10*S*-DOX), which was previously observed in Arctic sea ice and sinking particles (Amiraux et al., 2017; Rontani et al., 2018), and in estuaries of diverse latitudes (Galeron et al., 2018); however, the role of this enzyme in the environment has hitherto remained unclear. Here, we hypothesised that this enzyme could be employed by bacteria to detoxify free fatty acids released by wounded diatoms, perhaps as a result of increased copepod activity (i.e. grazing).

2. Experimental

2.1. Site description

The oceanographic time-series and marine biodiversity reference site L4 (50° 15′N, 4° 13′W, ca. 53 m water depth), is located in the Western English Channel, 13 km south southwest of

Plymouth, UK (Fig. 1). L4 is one of Europe's principal coastal time series sites and the Plymouth Marine Laboratory has sampled its natural phytoplankton community since 1992. The seasonal phytoplankton community at L4 has been well documented over many years (e.g. Widdicombe et al. 2010, Atkinson et al. 2015, Tarran and Bruun 2015, Cornwell et al. 2020). Specifically, phytoplankton biomass at L4 typically comprises a background population of flagellates, which increase steadily into summer (Atkinson et al 2015). A diatom bloom often begins in April, with a bloom of *Phaeocystis* spp. (Prymnesiophyte) in some years (Widdicombe et al 2010, Atkinson et al 2015). With the onset of summer stratification and nutrient limitation, Chl *a* levels often diminish around June as the diatom bloom is succeeded by a peak of autotrophic dinoflagellates (Atkinson et al 2015). Coccolithophores increase in the autumn of some years, but their contribution to biomass overall is relatively minor (Atkinson et al. 2015).

The microzooplankton protist assemblages are dominated by ciliates and colourless dinoflagellates (defined here as heterotrophic). Ciliates typically peak at around the same time as the spring diatom bloom (Widdicombe et al 2010, Atkinson et al 2015, Cornwell et al 2020), whereas the stronger peak of dinoflagellates appears later (Atkinson et al 2015). The non-carnivorous holoplankton, which also includes copepods, starts to increase before the spring bloom and is often sustained until October (Atkinson et al 2015). In contrast, the carnivorous zooplankton typically peak during the autumn (Atkinson et al., 2015).

2.2 SPM sampling

Water samples from 5 m and 25 m water depth were collected from the L4 station throughout 2018 (and some in 2019) on board the *R/V Plymouth Quest* (approximately monthly) using 10 L Niskin bottles mounted on to a conductivity, temperature and depth (CTD) rosette sampler. The particulate fractions were collected under subdued light conditions from 2-4 L of water by

means of vacuum filtration on 47 mm glass microfibre filters (Whatman, GF/F, as supplied). Water samples were processed immediately after collection and filtered materials kept frozen (-20°C) until further analysis.

2.3. Lipid extraction

Filtered water samples (GF/F filters) were reduced at room temperature with excess $NaBH_4$ (70 mg) after adding MeOH (25 mL, 30 min) to reduce labile hydroperoxides (resulting from photo- or autoxidation) to alcohols, which are more amenable to analysis by gas chromatography (GC). Water (25 mL) and KOH (2.8 g) were then added and the resulting mixture saponified by refluxing (2 h). After cooling, the mixture was acidified (HCl, 2 N) to pH 1 and extracted with dichloromethane (DCM; 3 × 20 mL). The combined DCM extracts were dried over anhydrous Na_2SO_4, filtered and concentrated by rotary evaporation at 40°C to give total lipid extracts (TLEs). TLEs were then silylated and analyzed by gas chromatography-electron impact quadrupole time-of-flight mass spectrometry (GC-QTOF). Analysis of blank filters showed the presence of small amounts (< 10% of the values obtained from water samples) of cholesterol and saturated fatty acids, which were subtracted.

A different treatment was used to determine the proportion of free fatty acids (FFAs). The samples were extracted three times with chloroform-MeOH-H_2O (1:2:0.8, v:v:v) using ultrasonication. The supernatant was separated by centrifugation at 3500G for 9 min. To initiate phase separation, purified H_2O was added to the combined extracts to give a final volume ratio of 1:1 (v:v). The upper aqueous phase was extracted three times with DCM and the combined DCM extracts were filtered and the solvent removed via rotary evaporation. The residue obtained after extraction was dissolved in 4 mL of DCM and separated into two equal subsamples. After evaporation of the solvent, fatty acids were directly quantified by GC-QTOF in the first subsample after silylation, while the second subsample was saponified and treated

as described above. Comparison of the amounts of fatty acids present before and after saponification enabled estimation of the percentage of FFAs. All the solvents (pesticide/glass distilled grade) and reagents (Puriss grade) were obtained from Rathburn and Sigma-Aldrich, respectively.

2.4. Silylation

Dry TLEs and standards were derivatized by dissolving them in 300 µL pyridine/bis-(trimethylsilyl)trifluoroacetamide (BSTFA; Supelco; 2:1, v/v) and silylated in a heating block (50 °C, 1 h). After evaporation to dryness under a stream of N_2, the derivatized residue was dissolved in ethyl acetate/BSTFA (2:1, v/v) (to avoid desilylation) and analysed by GC-QTOF.

2.5. Gas chromatography-EI quadrupole time-of-flight mass spectrometry

Accurate mass measurements were made in full scan mode using an Agilent 7890B/7200 GC/QTOF system (Agilent Technologies, Parc Technopolis – ZA Courtaboeuf, Les Ulis, France). A cross-linked 5% phenyl-methylpolysiloxane (Macherey-Nagel; OPTIMA-5MS Accent, 30 m × 0.25 mm, 0.25 µm film thickness) capillary column was used. Analyses were performed with an injector operating in pulsed splitless mode set at 270°C. Oven temperature was ramped from 70°C to 130°C at 20°C min^{-1} and then to 300°C at 5°C min^{-1}. The pressure of the carrier gas (He) was maintained at 0.69×10^5 Pa until the end of the temperature program. Instrument temperatures were 300°C for transfer line and 230°C for the ion source. Nitrogen (1.5 mL min^{-1}) was used as collision gas. Accurate mass spectra were recorded across the range *m/z* 50–700 at 4 GHz with the collision gas opened. The QTOF-MS instrument provided a typical resolution ranging from 8009 to 12252 from *m/z* 68.9955 to 501.9706. Perfluorotributylamine (PFTBA) was used for daily MS calibration. Compounds were

identified by comparing their TOF mass spectra, accurate masses and retention times with those of standards. Quantification of each compound involved extraction of specific accurate fragment ions, peak integration and determination of individual response factors using external standards and Mass Hunter (Agilent Technologies, Parc Technopolis – ZA Courtaboeuf, Les Ulis, France) software.

2.6. Standard compounds

Phytol (**12**), fatty acids, most of the sterols and 2,6,10,14-tetramethylpentadecanoic acid (pristanic acid) (**15**) were purchased from Sigma-Aldrich (St. Quentin Fallavier, France). 3,6-Dihydroxycholest-4-ene (**10**) (employed for sterol photooxidation estimates) was obtained from Maybridge Ltd. The synthesis of 3-methylidene-7,11,15-trimethylhexadecan-1,2-diol (phytyldiol) (**13**) was described by Rontani and Aubert (2005). 4,8,12-Trimethyltridecanoic acid (4,8,12-TMTD acid) (**16**) was synthesized from isophytol (**19**) (Interchim, Montluçon, France) by a previously described procedure (Rontani et al., 1991). 3,7,11,15-Tetramethylhexadecanoic acid (phytanic acid) (**14**) was produced in three steps from phytol (**12**) as described previously (Rontani et al., 2003). Cholestane-3β,5α,6β-triol (**11**) (employed for sterol autoxidation estimates) was produced by oxidation of cholesterol (**2**) with H_2O_2/KI/H_2SO_4 (Li and Li, 2013). (8-11)-Hydroperoxyhexadec-(8-10)-enoic acids (*Z* and *E*) (**30**-**35**) were produced by Fe^{2+}/ascorbate-induced autoxidation (Loidl-Stahlhofen and Spiteller, 1994) of palmitoleic acid (**23**). Subsequent reduction of these different hydroperoxides in methanol with excess $NaBH_4$ afforded the corresponding hydroxyacids. A standard of *threo* 7,10-dihydroxyoctadec-8(*E*)-enoic acid containing 10% of *threo* 7,10-dihydroxyhexadec-8(*E*)-enoic acid (**42**) previously produced by *Pseudomonas aeruginosa* PR3 (Suh et al., 2011) was obtained from Dr. H.R. Kim (School of Food Science and Biotechnology, Kyungpook National University, Daegu, Korea).

200

201 *2.7. Estimation of autoxidative, photooxidative and 10S-DOX degradation*

202 The role played by autoxidation, photooxidation and 10*S*-DOX oxidation in the degradation of
203 palmitoleic acid was estimated based on the profiles of isomeric allylic hydroxyacids obtained
204 after $NaBH_4$-reduction as described previously by Rontani et al. (2018).

205

206 **3. Results**

207

208 *3.1. Trophic environment at station L4 in 2018*

209 The main sterols in the filtered water samples: 24-norcholesta-5,22*E*-dien-3β-ol (24-norsterol)
210 (**1**), cholest-5-en-3β-ol (cholesterol) (**2**), cholesta-5,22*E*-dien-3β-ol (22-dehydrocholesterol)
211 (**3**), cholest-5,24-dien-3β-ol (desmosterol) (**4**), 24-methylcholesta-5,22*E*-dien-3β-ol (*epi*-
212 brassicasterol) (**5**), 24-methylcholesta-5,24(28)-dien-3β-ol (24-methylenecholesterol) (**6**), 24-
213 ethylcholest-5-en-3β-ol (sitosterol) (**7**), 24-ethylcholesta-5,22*E*-dien-3β-ol (fucosterol) (**8**) and
214 4α,23,24-trimethyl-5α-cholest-22*E*-en-3-ol (dinosterol) (**9**), were quantified to estimate the
215 nature and the amount of the algal material present in SPM samples across the 2018 time series.
216 At 5 m, sterol concentrations showed the occurrence of two peaks of phytoplanktonic biomass
217 at the end of April and in September (Table 1, Fig. 2A). In April, the sterol profile was
218 characterized by the presence of high percentages of cholesterol (**2**) and 24-norsterol (**1**), while
219 in September, cholesterol (**2**), brassicasterol (**5**), 24-methylenecholesterol (**6**) and dinosterol (**9**)
220 were the most abundant. At 25 m, two peaks of phytoplanktonic biomass could be observed at
221 the end of April and May (Table 2, Fig. 2B) with the percentages of cholesterol (**2**) and 24-
222 norsterol (**1**) again relatively abundant during these two events. A relatively high abundance of
223 brassicasterol (**5**) was also observed at 25 m in May.

At 25 m, the concentration of phytol (chlorophyll phytyl side-chain) (**12**) followed logically the same trend as that of the sterols (Table 2). In contrast, we observed a small lag between the date of the highest concentration of phytol (**12**) (08/13/18) and total sterols (09/17/18) at 5 m (Table 1). Concerning isoprenoid acids, a peak in phytanic acid (**14**) concentration was detected on 04/30/18 at both depths, while highest 4,8,12-TMTD acid (**16**) concentrations were observed in February and March at 5 m (Tables 1 and 2, Fig. 3).

We also quantified the main saturated (SFAs), monounsaturated (MUFAs) and polyunsaturated (PUFAs) fatty acids (Tables 3 and 4). While SFAs appeared to be dominant and the percentage of MUFAs relatively constant at both depths across the 2018 time series, PUFAs were highly variable at both depths. SFAs were dominated by $C_{16:0}$ (**21**) and $C_{14:0}$ (**20**), MUFAs by $C_{16:1\omega9}$ (palmitoleic acid) (**22**) and $C_{18:1\omega9}$ (oleic acid) (**24**), and PUFAs by $C_{20:5}$ (**26**) and $C_{22:6}$ (**27**). The bacterially-derived $C_{18:1\omega7}$ (*cis*-vaccenic acid) (**25**) and branched (*iso* and *anteiso*) $C_{15:0}$ acids ($BrC_{15:0}$) (**28** and **29**) were also detected.

3.2. Biotic and abiotic degradation of lipid components of phytoplankton at station L4 in 2018

3.2.1. Photooxidation

Due to the higher solar irradiance available, it is perhaps not surprising that photooxidation processes acted more intensively at 5 m than at 25 m, although only the most reactive lipids (e.g. chlorophyll) appeared to be strongly affected by this process (Tables 1 and 2, Fig. 4). Thus, chlorophyll photooxidation estimates were highly variable at 5 m (ranging from 8% to 100%) (Table 1, Fig. 4) yet relatively consistent and low at 25 m (10%–26%) (Table 2). The photooxidation of MUFAs (reaching 2.4% and 2.0% at 5 m and 25 m, respectively) was very limited at both depths (Fig. 5), while Δ^5-sterols appeared to be essentially unaffected.

249 *3.2.2. Autoxidation*

250 3,7,11,15-tetramethylhexadec-3(*cis*/*trans*)-ene-1,2-diols (**17**) and 3,7,11,15-tetramethyl-
251 hexadec-2(*cis*/*trans*)-ene-1,4-diols (**18**) resulting from autoxidation of the chlorophyll phytyl
252 side-chain could be identified in the different samples investigated, but were not quantified.
253 Similarly, the detection of *cis*-hydroxyhexadecenoic acids (**40** and **41**, see appendix) provides
254 evidence for autoxidation of palmitoleic acid (**22**), although this was relatively minor, reaching
255 only a maximum of 14% and 16% in January at 5 and 25 m, respectively (Fig. 5). In contrast,
256 autoxidation products of Δ^5-sterols (i.e. 3β,5α,6β-steratriols; Rontani, 2012) were not detected
257 in any of the samples.

258

259 *3.2.3. Biotic degradation*

260 A clear dominance of 10-hydroxyhexadec-8(*E*)-enoic acid (**36**) was observed within the
261 palmitoleic acid oxidation products in the sample collected on 04/30/18 at 25 m (Fig. 6B), and
262 attributed to the involvement of a bacterial 10-dioxygenase enzyme (10*S*-DOX). Similar
263 evidence for the involvement of this enzyme was also observed in the corresponding sample
264 collected at 5 m, but in this case 8-hydroxyhexadec-9(*E*)-enoic acid (**38**) was also dominant
265 (Fig. 6A). 10*S*-DOX degradation of palmitoleic acid (**22**) in these samples was estimated to be
266 27% and 25% at 5 m and 25 m, respectively (Fig. 5A and 5B). Analysis of samples collected
267 in 2019, albeit from 25 m water depth only, provides further indication of the seasonal nature
268 of this bacterial activity at the L4 station (10*S*-DOX degradation of palmitoleic acid reaching
269 6% in April; Rontani et al., unpublished data), although multi-annual studies are needed to
270 confirm this.

271 Quantification of the free fatty acid (FFA) content in the sample collected on 04/30/18 at
272 5 m showed a very high proportion of free palmitoleic (**22**) and $C_{20:5}$ (**26**) acids (76% and 74%,
273 respectively). Interestingly, *threo* 7,10-dihydroxyhexadec-8(*E*)-enoic acid (**42**) could also be

identified in these samples by comparison of its accurate mass spectrum and retention time with those of a reference compound (Fig. S1). A slightly later eluting compound (Fig. S1), exhibiting the same mass spectrum as *threo* 7,10-dihydroxyhexadec-8(*E*)-enoic acid (**42**), was identified as a mixture of the *erythro* diastereoisomers of this diol (**43**). Such an elution order is in good agreement with the results of Hansel and Evershed (2009).

4. Discussion

4.1. Trophic environment at station L4 in 2018

Sterols possess structural characteristics, such as double bond positions, nuclear methylation and patterns of side-chain alkylation, which are restricted to a few groups of organisms (for reviews see Volkman, 1986; 2003; Rampen et al., 2010). These lipids are thus often used to estimate phytoplanktonic diversity (e.g. Veron et al., 1998; Taipale et al., 2016). For example, 24-norsterol (**1**) has previously been identified as a characteristic sterol in diatoms, both in culture of the centric diatom *Thalassiosira antarctica* (Rampen et al., 2007) and in the environment (e.g. Suzuki et al., 2005). The relatively high proportions of 24-norsterol (**1**) observed in our SPM samples collected on 04/30/18 at 5 m and 25 m (30% and 20% of total sterols, respectively) (Tables 1 and 2), along with relatively high values of the diatom fatty acid ratio (($C_{14:0}$ + $C_{16:1\omega7}$ + ΣC_{16} PUFAs)/$C_{16:0}$) (Léveillé et al., 1997) and the diatom-specific $C_{20:5}$ FA (Tables 3 and 4), thus suggest a strong contribution from diatoms during this period. Indeed, our lipid data are consistent with previous taxonomic results of Cornwell et al. (2020), who showed that diatom biomass increased strongly (more than fourfold) between weeks 16 and 18 of 2018 (corresponding to our 04/19/18 and 04/30/18 samples, respectively). In particulate matter, the (MUFAs + PUFAs)/SFAs ratio varies generally from 0.6 during the initial and lag phases of phytoplankton blooms to greater than 1.0 at high rates of organic production (Marty

et al., 1988; Mayzaud et al., 1989). The high values observed on 04/30/18 and 05/30/18 at 25 m (1.7 and 1.2, respectively), accompanied by elevated values of $C_{20:5}$ FA (Table 4), are thus also consistent with the occurrence of diatom blooms on these dates (Cornwell et al., 2020). Interestingly, Widdicombe et al. (2010) previously observed a shift in phytoplankton composition at the L4 station between late March and early May from a winter community (dominated by centric and benthic diatoms) towards a community dominated by *Chaetoceros* spp., *Thalassiosira* spp. (potential sources of 24-norsterol, Rampen et al., 2007) and *Skeletonema costatum*.

On the basis of the relatively high abundance of brassicasterol (**5**) in the 25 m sample collected in May (Table 2, Fig. 2), a significant contribution of *Phaeocystis* could be inferred (Nichols et al., 1991), as is frequently the case at the L4 station during April/May (Widdicombe et al., 2010).

Dinoflagellates are important primary producers in the oceans (Kokke et al., 1982), differing from other classes of marine algae with respect to the dominance of 4α-methylsterols among their sterols. Dinosterol (**9**), for example, which is the major sterol in several dinoflagellates (Shimizu et al., 1976; Kokke et al., 1982), is often employed as tracer for the contribution of these organisms in the marine environment (Robinson et al., 1984). The significant proportion of this sterol in the 09/17/18 sample at 5 m (Fig. 2), along with relatively elevated concentrations of the $C_{22:6}$ FA (produced in high proportion by several dinoflagellates, Peltomaa et al., 2019) (Table 3), thus suggests an important contribution of dinoflagellates to this bloom event, consistent with the results of Cornwell et al. (2020), who identified a peak in ellipsoid-shaped dinoflagellates between weeks 36 and 38 (Sept 2018) at 10 m water depth.

The lag between the highest concentrations of phytol (**12**) (08/13/18) and sterols (09/17/18) at 5 m (Table 1), can be attributed to the presence of a bloom of cyanobacteria (well-known to contain very low proportions of sterols; Volkman, 2003) at the end of August, as also

supported by the observations of Cornwell et al. (2020), who showed the presence of a single biomass maximum of *Synechoccocus* at the L4 station during the same period.

Pelagic crustaceans assimilate the chlorophyll phytyl chain when feeding herbivorously (for a review see Rontani and Volkman, 2003). Phytanic acid (**14**), which arises from hydrogenation and terminal oxidation of phytol (**12**), is an important lipid in species of *Calanus* (Blumer and Cooper, 1967; Avigan and Blumer, 1968; Prahl et al., 1984). Classical oxidative metabolism of this isoprenoid acid (Mize et al., 1969) affords pristanic (**15**) and 4,8,12-TMTD (**16**) acids, which have also been detected in different *Calanus* species (Avigan and Blumer, 1968; Prahl et al., 1984). These three isoprenoid acids may also be produced during the biodegradation of phytol (**12**) by marine bacteria (Rontani et al., 1999). The high concentrations of phytanic acid (**14**) observed at the end of April at 5 m and 25 m (Fig. 3) therefore strongly suggests the presence of a high proportion of copepods, evident also from a high proportion of cholesterol (**2**) in these samples (Fig. 2). Indeed, herbivorous crustaceans use common dietary algal sterols such as *epi*-brassicasterol (**5**) or 24-methylenecholesterol (**6**) to synthesize cholesterol (**2**) via dealkylation and reduction (Grieneisen, 1994; Behmer and Nes, 2003). The weak proportion of desmosterol (**4**) (an intermediate in the conversion of dietary phytosterols to cholesterol (**2**) by copepods; Goad 1978) observed in the April samples likely reflects the highly efficient conversion of phytosterols to cholesterol (**2**) by copepods, with little accumulation of desmosterol (**4**) (Cass et al., 2011). The presence of a high proportion of copepods inferred from the sterol composition in April further aligns with the results of Cornwell et al. (2020) who conducted a 1-year intensive study of the copepod *Oithona similis* at the L4 station over the 2017–2018 season. Thus, increasing abundances of *O. similis* were identified during the same period as the elevated cholesterol levels in our SPM samples (i.e. between weeks 15 and 19 of 2018) (Cornwell et al., 2020), together with an increase in fecal pellets in the phytoplankton community (phytoplankton net, 20 µm mesh size) (Widdicombe,

personal communication). Indeed, increased copepod grazing and feeding on diatoms are common occurrences during the spring bloom at L4 (e.g. Bautista and Harris (1992), Harris et al. (2000)).

In summary, biomarker analysis of the SPM samples provide valuable background information about the trophic environment at L4 during 2018. Specifically, elevated contributions from diatoms and *Phaeocystis* could be identified during the spring, along with copepods. On the other hand, the late summer/autumn biomarker pool provides evidence for an environment dominated by dinoflagellates, with some contribution from cyanobacteria. These lipid data are also in very good agreement with recent and long-term studies of trophic environments at L4 (e.g. Cornwell et al 2020, Atkinson et al 2015, Widdicombe et al 2010, Eloire et al 2010).

4.2. Biotic and abiotic degradation of lipid components of phytoplankton at station L4 in 2018

4.2.1. Photooxidation

Due to the presence of chlorophylls, which are very efficient photosensitizers (Foote, 1976; Knox and Dodge, 1985), unsaturated lipid components of phytoplankton are susceptible to Type II photosensitized oxidation (i.e. involving singlet oxygen ($^1O_2$)) processes (Rontani and Belt, 2020). The efficiency of these processes is strongly dependent on: (i) the residence time of cells within the euphotic layer (Zafiriou et al., 1984; Mayer et al., 2009), and (ii) the physiological state of phytoplanktonic cells (Merzlyak and Hendry, 1994; Nelson, 1993). Indeed, $^1O_2$ production can exceed the quenching capacities of the photoprotective system (and thus induce cell damage) only when the photosynthetic pathways are not operative as is the case of senescent or highly stressed cells (Nelson, 1993).

Based on its high specificity and widespread occurrence in the environment (Cuny and Rontani, 1999), 3-methylidene-7,11,15-trimethylhexadecan-1,2-diol (phytyldiol) (**13**) produced during Type II photosensitized oxidation of the chlorophyll phytyl side-chain (Rontani et al., 1994), was proposed previously as a specific and stable tracer of chlorophyll photodegradation (Cuny et al., 2002). The molar ratio phytyldiol (**13**)/phytol (**12**) is often referred to as the Chlorophyll Phytyl side-chain Photodegradation Index (CPPI) and provides a useful semi-quantitative estimate for photodegradation of all chlorophylls with a phytyl side-chain in the marine environment (Cuny et al., 2002). Interestingly, in our SPM samples, the highest chlorophyll photo-oxidation estimates at 5 m mirror the two bloom events and are strongly anti-correlated to the concentration of phytol (**12**) (and therefore of chlorophyll) (Fig. 4) ($R^2 = 0.81$, n = 14), indicating that photooxidation processes act before and after the blooms on old or senescent cells, but not on healthy cells during the blooms.

Unsaturated fatty acids, which generally predominate in the photosynthetic membranes of algae (Woods, 1974), may also be strongly affected by Type II photosensitized oxidation processes in senescent phytoplanktonic cells (Rontani and Belt, 2020). The photodegradation rates of these compounds logically increase with their degree of unsaturation (Rontani et al., 1998), rendering PUFAs, in particular, very reactive towards these processes (Frankel, 1998; Rontani et al., 1998). Based on the correspondence between the lowest proportions of PUFAs and the highest chlorophyll photooxidation estimates at 5 m (Fig. 4), the involvement of Type II photosensitized oxidation processes in PUFA degradation would be expected, yet no PUFA photooxidation products were detected. This is possibly due to: (i) the instability of the polyunsaturated hydroperoxides formed, or (ii) the involvement of intermolecular cross-linking reactions leading to the formation of compounds with macromolecular structures (Neff et al., 1988), which are not readily analyzed by gas chromatography. Exceptionally, for the sample collected on 01/22/18 at 5 m, where chlorophyll photooxidation % and the proportion of PUFAs

were both low (Fig. 4), PUFA degradation seems to result from autoxidation processes (see section 4.2.2).

Type II photosensitized oxidation of Δ^9 MUFAs produces similar proportions of 9- and 10-hydroperoxides with an allylic *trans*-double bond (Frankel et al. 1979; Frankel, 1998), which can subsequently undergo stereoselective radical allylic rearrangement to 11-*trans* and 8-*trans* hydroperoxides, respectively (Porter et al. 1995). In contrast, MUFA autoxidation results mainly in the formation of 9-*trans*, 10-*trans*, 11-*trans*, 11-*cis*, 8-*trans* and 8-*cis* hydroperoxides (Frankel, 1998). Autoxidative processes can be readily characterised after $NaBH_4$-reduction due to the formation of *cis* allylic hydroxyacids, which are specific products of these degradation processes (Porter et al., 1995; Frankel, 1998). The contribution of hydroxyacids resulting from autoxidative processes may be distinguished from that arising from photooxidative processes according to the proportions of *cis*-hydroxyacids detected and the water temperature (Frankel, 1998; Marchand and Rontani, 2001). The results obtained here showed only a very weak photooxidation of palmitoleic acid (**22**) (the main MUFA present in the samples) at both depths (Fig. 5).

Finally, as important unsaturated components of biological membranes, Δ^5-sterols are also susceptible to photooxidative degradation during the senescence of phytoplankton (Rontani and Belt, 2020). However, their photodegradation is generally slower than that of MUFAs due to steric hindrance between the sterol Δ^5 double bond and $^1O_2$ (Beutner et al., 2000). The failure to detect photooxidation products of Δ^5-sterols is therefore consistent with the very weak photodegradation of MUFAs (Tables 3 and 4). During the time series investigated, Type II photosensitized oxidation thus seems to have acted most intensively only on the more reactive lipids (i.e. chlorophyll and PUFAs).

4.2.2. Autoxidation

3,7,11,15-tetramethylhexadec-3(*cis*/*trans*)-ene-1,2-diols (**17**) and 3,7,11,15-tetramethyl-hexadec-2(*cis*/*trans*)-ene-1,4-diols (**18**) were previously proposed as indicators of radical-mediated oxidative degradation of the chlorophyll phytyl side-chain in the environment (Rontani and Aubert, 2005), and were indeed detected in the current water column samples. Unfortunately, despite the high specificity and widespread occurrence of these diols in the environment, the formation of several additional labile oxidation products during the autoxidation of the phytyl side-chain (Rontani et al., 2003) prevented semi-quantitative estimation of chlorophyll autoxidation.

Although more intense than photooxidation, autoxidation of palmitoleic acid (**22**) was relatively low during the time series (Fig. 5). It may be noted that the autoxidation percentages (ranging from 0 to 16%) are clearly in the low range previously observed in polar, tropical and temperate regions (for a review see Rontani and Belt, 2020). Highest autoxidation (14.2 and 16.2% at 5 and 25 m, respectively) was observed in January (Fig. 5), suggesting that autoxidative processes also likely played an important role in the degradation of PUFAs at that time (Fig. 4). Indeed, PUFAs such as $C_{20:5}$ (**26**) are autoxidized at a rate more than one order of magnitude faster than MUFAs in senescent diatom cells (Rontani et al., 2014). It was proposed previously that the induction of autoxidative processes in phytodetritus derives likely from the cleavage of photooxidative hydroperoxides (Girotti, 1998; Rontani et al., 2003) so it might be expected that high rates of autoxidation would correspond to high rates of photooxidation. This is clearly not the case in January, when the autoxidation state of MUFAs was the highest (Fig. 5) and chlorophyll photooxidation (%) was the lowest (Fig. 4), probably because the intensity of autoxidative processes depends not only on the quantity of photochemically-produced hydroperoxides present in the cells, but also on conditions favouring their homolytic cleavage (e.g. the presence of LOXs or redox-active metal ions, heat or light; Sheldon and Kochi, 1976; Schaich, 2005).

Autoxidation of Δ^5-sterols is generally slower than that of MUFAs in senescent diatom cells (Rontani et al., 2014). Since the extent of MUFA autoxidation was relatively low in the SPM samples (Fig. 5), the very weak autoxidation of sterols was as expected. Therefore, as seen for Type II photosensitized oxidation, autoxidation seems to have acted mainly on the most reactive lipids (i.e. chlorophyll and PUFAs).

4.2.3. Biotic degradation

Type II photosensitized oxidation and free-radical induced oxidation of Δ^9 MUFAs such as palmitoleic acid (**22**) produce (after $NaBH_4$-reduction of hydroperoxyacids) equal proportions of the major 9-*E* and 10-*E* isomeric allylic hydroxyacids (**36** and **37**) (Frankel, 1998). The strong predominance of 10-hydroxyhexadec-8(*E*)-enoic acid (**36**) observed in the SPM samples collected on 04/30/18 (Fig. 6) can thus be attributed to the involvement of a specific biotic oxidation process. A similar dominance of this isomer among palmitoleic acid (**22**) oxidation products was observed previously in sea ice and in sinking particles in the Canadian Arctic (Amiraux et al., 2017; Rontani et al., 2018), and also in estuaries of diverse latitudes (Galeron et al., 2018). Its occurrence has previously been attributed to the involvement of specific bacterial dioxygenase activity and to a 10*S*-DOX enzyme, in particular. Indeed, a 10*S*-DOX enzyme capable of converting palmitoleic acid (**22**) to 10(*S*)-hydroperoxyhexadec-8(*E*)-enoic acid (**30**) (reduced to the corresponding hydroxyacid during $NaBH_4$-reduction) was previously isolated from the bacteria *Pseudomonas aeruginosa* 42A2 (Guerrero et al., 1997; Busquets et al., 2004) and, more recently, found in other genera of marine bacteria, namely *Pseudoalteromonas*, *Shewanella* and *Aeromonas* (Shoja Chaghervand, 2019). The involvement of 10*S*-DOX enzymatic activity in these SPM samples is further supported by detection of *threo* 7,10-dihydroxyhexadec-8(*E*)-enoic acid (**42**) (Fig. S1), formed from the specific action of 7*S*,10*S*-hydroperoxide diol synthase (linked to the 10*S*-DOX enzymatic activity) (Estupiñán et

al., 2014; 2015) on 10(*S*)-hydroperoxyhexadec-8(*E*)-enoic acid (**30**) (Fig. 7). It may be noted that isomerization of the latter by hydroperoxide isomerases (Fig. 7), which are well known to produce *erythro* allylic 1-4 diols (Jernerén et al., 2010), may explain the observed formation of the *erythro* 7,10-dihydroxyhexadec-8(*E*)-enoic acids (**43**) (Fig. S1).

Martinez et al. (2010) previously suggested that fatty acids bind to bacterial 10*S*-DOX via their carboxyl groups at a fixed position relative to the catalytic site. This enzyme, localized in the periplasm (Martinez et al., 2013), should thus be mainly active on FFAs and therefore contribute to the detoxification of these deleterious fatty acids (Monfort et al., 2000; Desbois and Smith, 2010) in the bacterial environment (Martínez et al., 2010). The very high proportions of FFAs (and most notably of palmitoleic acid (**22**)) measured in the SPM samples exhibiting the highest 10*S*-DOX activity certainly supports this hypothesis. Further, the trophic level in April 2018 was characterised by: (i) the dominance of diatoms (notably of *Thalassiosirales*) and (ii) the presence of a very high copepod activity (see Section 4.1).

Interestingly, an oxylipin-based chemical defence against copepods was observed previously in the diatom *Thalassiosira rotula* (Pohnert 2000; 2002), being initiated by phospholipases acting immediately after cell damage. This lipase activity leads to the preferential release of free MUFAs and PUFAs, the latter converted further by lipoxygenases to reactive defensive metabolites such as the antiproliferative PolyUnsaturated Aldehydes (PUAs) (Fig. 8), which are well-known to inhibit egg cleavage in copepods (Miralto et al.,1999). In contrast, free MUFAs, which are not affected by lipoxygenases, are released intact outside of wounded diatoms. These compounds (dominated by palmitoleic acid (**22**) in diatoms, Pedersen et al., 1999) exhibit a strong bactericidal action towards marine Gram-negative pathogens (Desbois et al., 2009; Desbois and Smith, 2010). The strong 10*S*-DOX bacterial activity observed in SPM samples in April (Fig. 5) can therefore be attributed to a detoxification strategy allowing bacteria associated to diatoms grazed by copepods to survive the release of

bactericidal free palmitoleic acid (**22**) (Fig. 8). 10(*S*)-Hydroperoxyhexadec-8(*E*)-enoic and *threo* 7,10-dihydroxyhexadec-8(*E*)-enoic acids (**30** and **42**) resulting from 10*S*-DOX and diol synthase activities, respectively, may be then transported from the periplasmic space of bacteria to the external medium (Martinez et al., 2013).

9- and 10-hydroperoxyacids with an allylic *E* double bond can undergo highly stereoselective allylic rearrangement to 11-*E* and 8-*E* hydroperoxides, respectively (Fig. 7), the extent of which increases with time (Porter et al., 1995). A lower proportion of the 8-*E* isomer observed in the SPM sample collected on 04/30/18 from 25 m depth (10-*E*/8-*E* = 4.5 vs 10-*E*/8-*E* = 1.2 at 5 m) (Fig. 6) thus suggests an involvement of the 10*S*-DOX activity at 25 m and an aging of material collected from a shallower 5 m depth. The highest abundance of the copepod *O. similis* at 25 m observed by Cornwell et al. (2020) likely indicates a strong alteration of diatoms and thus an enhanced production of FFAs, which in turn supports an induction of the bacterial 10*S*-DOX activity at this depth. The ascent of planktonic and bacterial material from 25 m to 5 m can be facilitated by the presence of a high proportion of Transparent Exopolymer Particles (TEPs) in the shallower SPM, formed abiotically from dissolved precursors released by phytoplankton and bacteria (Passow, 2000) and composed mainly of surface-active polysaccharides (Mopper et al., 1995). Due to their positive buoyancy, TEPs can provide a means for the upward flux of bacteria and phytoplankton in the marine environment (Azetsu-Scott and Passow, 2004).

Allylic rearrangement of hydroperoxides in biological membranes is strongly sensitive to the hydrogen atom donor properties of their surrounding molecules (Porter et al., 1994; 1995). In algal membranes containing a high proportion of PUFAs, which are good hydrogen atom donors, allylic rearrangement should be weak (Fig. 7). In contrast, in bacterial periplasm containing only SFAs and MUFAs (both weak hydrogen atom donors), the rearrangement should be favoured (Fig. 7). The extent of the allylic rearrangement of the different

hydroperoxides present in each sample therefore reflects the composition of the organisms (bacteria or phytoplankton) present. The strong allylic rearrangement of 10*S*-hydroperoxyhexadec-8(*E*)-enoic acid (**30**) to 8-hydroperoxyhexadec-9(*E*)-enoic acid (**32**) observed in the SPM sample collected at 5 m on 04/30/18 (Fig. 6A) thus provides further evidence for 10*S*-DOX activity in the bacterial periplasm. Interestingly, in the same samples, the rearrangement of 9-hydroperoxyhexadec-10(*E*)-enoic acid (**31**) (produced abiotically in senescent algae) to the corresponding 11-hydroperoxyhexadec-9(*E*)-enoic acid (**33**) appeared to be only very weak (Fig. 6A).

5. Conclusions

Selected lipids (sterols and fatty acids) and their biotic and abiotic oxidation products were quantified in SPM samples collected mainly in 2018 from two depths (5 m and 25 m) at the marine time series station L4 located in the western English Channel. The sterol and fatty acid composition was typical of mixed trophic communities at L4 throughout 2018, with a seasonal evolution from mainly diatoms and copepods in spring to dinoflagellates in late summer/autumn, consistent with recent and long-term taxonomic studies.

Abiotic lipid autoxidation and photodegradation were both found to be relatively minor, acting mainly on the most reactive lipids. A slightly greater influence of abiotic degradation, however, was found at 5 m compared to 25 m, likely due to higher irradiance and ascent of older planktonic/bacterial material from deeper to shallower waters.

In contrast, significant biotic degradation was evident in samples collected at the end of April. In particular, we observed a strong predominance of certain hydroxyacids linked to specific biotic oxidation process involving bacterial dioxygenase (10*S*-DOX) activity. This contribution from 10*S*-DOX in samples at the end of April was accompanied by a relatively high proportion of FFAs, likely resulting from a chemically-induced defense mechanism by

diatoms during times of increased zooplankton (copepod) activity. Since FFAs (dominated by palmitoleic acid in diatoms) exhibit a strong bactericidal action towards marine pathogens such as bacteria, the strong 10S-DOX bacterial activity observed in the April SPM samples points to a detoxification strategy by bacteria against the production of bactericidal free palmitoleic acid (**22**). We thus propose that this enzyme could be employed by bacteria to detoxify FFAs released by wounded diatoms in the presence of copepods.

Acknowledgements

We thank Louise Elizabeth Cornwell for providing us with some of the data from the Cornwell et al (2020) study. We also thank the crew of the RV Plymouth Quest for collection of samples used in this study. Financial support from the Centre National de la Recherche Scientifique (CNRS) and the Aix-Marseille University is gratefully acknowledged. Thanks are also due to the FEDER OCEANOMED (No. 1166-39417) for the funding of the GC-QTOF employed. Claire Widdicombe was funded through the UK Natural Environment Research Council's National Capability Long-term Single Centre Science Programme, Climate Linked Atlantic Sector Science, grant number NE/R015953/1, and is a contribution to Theme 1.3 - Biological Dynamics. We acknowledge Remi Amiraux for assistance with generating the schematic of 10*S*-DOX activity. We are also grateful to two anonymous reviewers for their useful and constructive comments.

APPENDIX

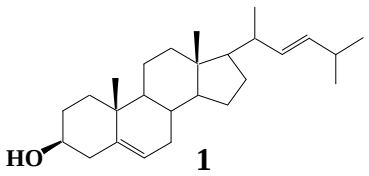

1

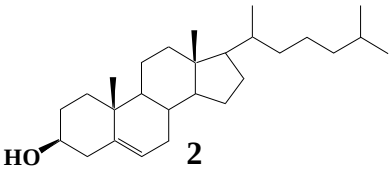

2

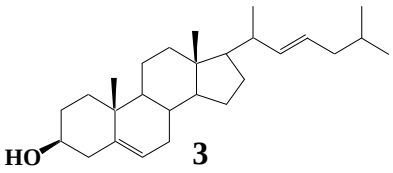

3

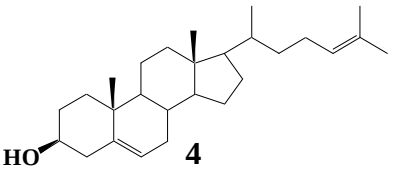

4

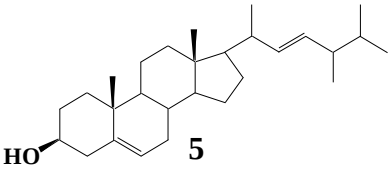

5

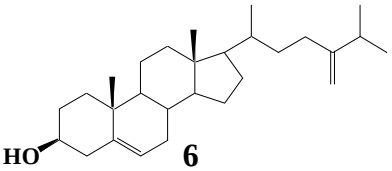

6

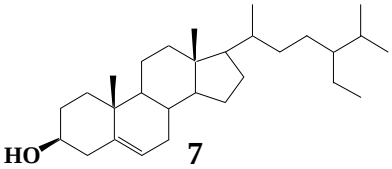

7

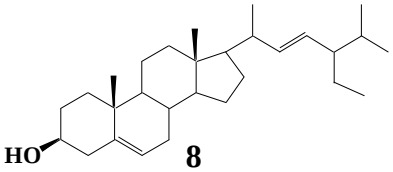

8

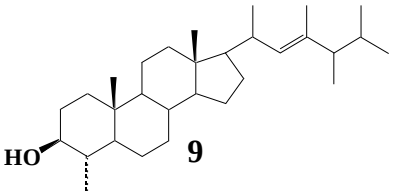

9

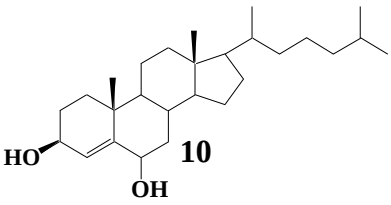

10

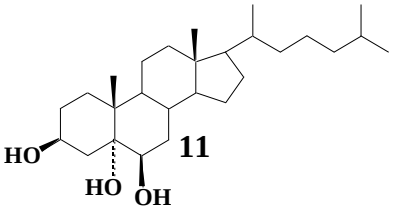

11

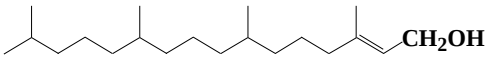

12

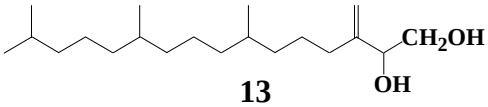

13

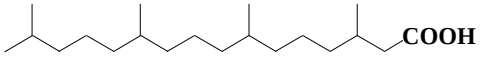

14

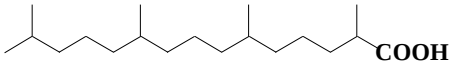

15

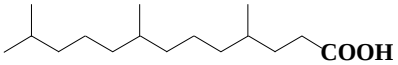

16

568

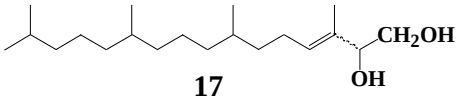

17

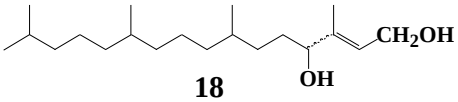

18

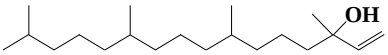

19

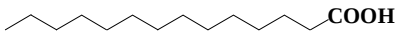

20

21

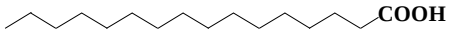

22

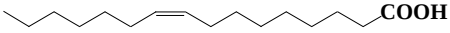

23

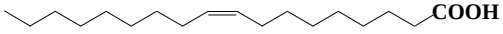

24

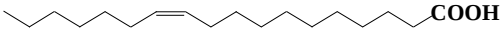

25

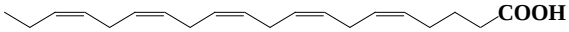

26

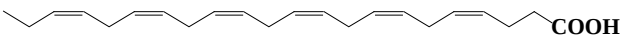

27

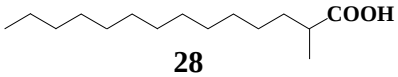

28

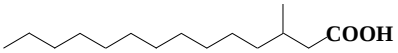

29

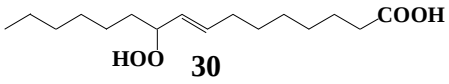

30

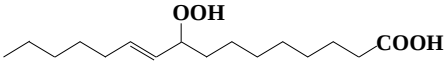

31

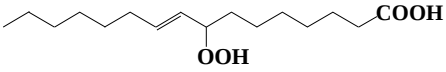

32

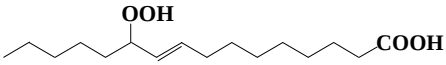

33

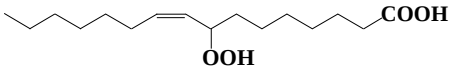

34

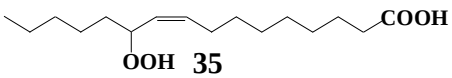

35

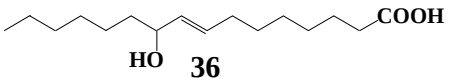

36

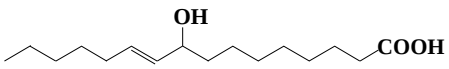

37

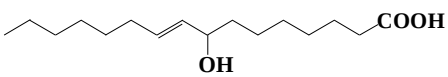

38

569

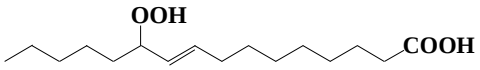

39

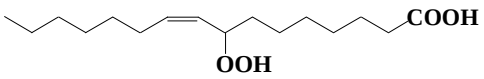

40

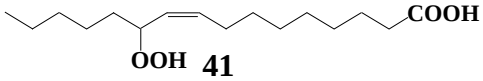

41

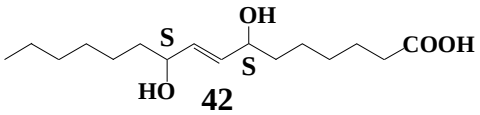

42

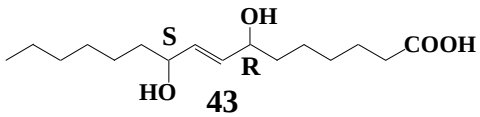

43

570

References

Amiraux, R., Belt, S.T., Vaultier, F., Galindo, V., Gosselin, M., Bonin, P., Rontani, J.-F., 2017. Monitoring photo-oxidative and salinity-induced bacterial stress in the Canadian Arctic using specific lipid tracers. Mar. Chem. 194, 89–99. doi.org/10.1016/j.marchem.2017.05.006

Atkinson, A., Harmer, R.A., Widdicombe, C.E., McEvoy, A.J., Smyth, T.J., Cummings, D.G., Somerfield, P.J., Maud, J.L., McConville, K., 2015. Questioning the role of phenology shifts and trophic mismatching in a planktonic food web. Progr. Oceanogr. 137, 498–512. doi.org/10.1016/j.pocean.2015.04.023

Avigan, J., Blumer, M., 1968. On the origin of pristane in marine organisms. J. Lipid Res. 9, 350–352.

Azetsu-Scott, K., Passow, U., 2004. Ascending marine particles: Significance of transparent exopolymer particles (TEP) in the upper ocean. Limnol. Oceanogr. 49, 741–748. doi.org/10.4319/lo.2004.49.3.0741

Bacon, M.P., Huh, C.-A., Fleer, A.P., Deuser, W.G., 1985. Seasonality in the flux of natural radionuclides and plutonium in the deep Sargasso Sea. Deep Sea Res. Part A. 32, 273–286. doi.org/10.1016/0198-0149(85)90079-2

Bautista, B., Harris, R. P., 1992. Copepod gut contents, ingestion rates and grazing impact on phytoplankton in relation to size structure of zooplankton and phytoplankton during a spring bloom. Marine Ecology Progress Series, 82, 41-50.

Behmer, S.T., Nes, W.D., 2003. Insect sterol nutrition and physiology: a global overview. Adv. Insect Physiol. 31, pp.1–72. doi.org/10.1016/S0065-2806(03)31001-X

Beutner, S., Bloedorn, B., Hoffman, T., Martin, H.D., 2000. Synthetic singlet oxygen quenchers. In: Packer, L., Sies, H. (Eds.), Methods in Enzymology, vol. 319. Academic Press, New York, pp. 226–241. doi.org/10.1016/S0076-6879(00)19024-X

Blumer, M., Cooper, W. J., 1967. Isoprenoid Acids in Recent Sediments. Science 158, 1463–1464. doi.org/10.1126/science.158.3807.1463

Busquets, M., Deroncelé, V., Vidal-Mas, J., Rodríguez, E., Guerrero, A., Manresa, A., 2004. Isolation and characterization of a lipoxygenase from *Pseudomonas* 42A2 responsible for the biotransformation of oleic acid into (*S*)-(*E*)-10-hydroxy-8-octadecenoic acid. Antonie Van Leeuwenhoek 85, 129–139. doi.org/10.1023/B:ANTO.0000020152.15440.65

Cass, C.J., Wakeham, S.G., Daly, K.L., 2011. Lipid composition of tropical and subtropical copepod species of the genus *Rhincalanus* (Copepoda: Eucalanidae): a novel fatty acid and alcohol signature. Mar. Ecol. Progr. Ser. 439, 127–138. doi.org/10.3354/meps09324

618 Cuny, P., Rontani, J.-F., 1999. On the widespread occurrence of 3-methylidene7,11,15-
619 trimethylhexadecan-1,2-diol in the marine environment: a specific isoprenoid marker of
620 chlorophyll photodegradation. Mar. Chem. 65, 155–165. doi.org/10.1016/S0304-
621 4203(98)00093-0
622
623 Cuny, P., Marty, J.-C., Chiaverini, J., Vescovali, I., Raphel, D., Rontani, J.-F., 2002. One year
624 seasonal survey of the chlorophyll photodegradation process in the Northwestern
625 Mediterranean Sea. Deep-Sea Res. II 49, 1987–2005. doi.org/10.1016/S0967-
626 0645(02)00023-1
627
628 Cornwell, L.E., Fileman, E.S., Bruun, J.T., Hirst, A.G., Tarran, G.A., Findlay, H.S., Lewis, C.,
629 Smyth, T.J., McEvoy, A.J., Atkinson, A., 2020. Resilience of the Copepod *Oithona*
630 *similis* to Climatic Variability: Egg Production, Mortality, and Vertical Habitat
631 Partitioning. Front. Mar. Sci. 7:29. doi.org/10.3389/fmars.2020.00029
632
633 Desbois, A.P., Smith, V.J., 2010. Antibacterial free fatty acids: activities, mechanisms of action
634 and biotechnological potential. Appl. Microbiol. Biotechnol. 85, 1629–1642.
635 doi.org/10.1007/s00253-009-2355-3
636
637 Desbois, A.P., Mearns-Spragg, A., Smith, V.J., 2009. A Fatty acid from the diatom
638 *Phaeodactylum tricornutum* is antibacterial against diverse bacteria including multi-
639 resistant *Staphylococcus aureus* (MRSA). Mar. Biotechnol. 11, 45–52.
640 doi.org/10.1007/s10126-008-9118-5
641

642 Eloire, D., Somerfield, P. J., Conway, D. V. P., Halsband-Lenk, C., Harris, R.Bonnet, D., 2010.
643 Temporal variability and community composition of zooplankton at station L4 in the
644 Western Channel: 20 years of sampling. Journal of Plankton Research, 32, 657-679.
645 doi.org/10.1093/plankt/fbq009
646
647 Estupiñán, M., Diaz, P., Manresa, A., 2014. Unveiling the genes responsible for the unique
648 *Pseudomonas aeruginosa* oleate-diol synthase activity. Biochim. Biophys. Acta 1841,
649 1360–1371. doi.org/10.1016/j.bbalip.2014.06.010
650
651 Estupiñán, M., Álvarez-García, D., Barril, X., Diaz, P., Manresa, A., 2015. *In silico/ in vivo*
652 insights into the functional and evolutionary pathway of *Pseudomonas aeruginosa* oleate-
653 diol synthase. Discovery of a new bacterial di-heme cytochrome C peroxidase subfamily.
654 PLoS One 10(7): e0131462. doi.org/10.1371/journal.pone.0131462Foote, C.S., 1976.
655 Photosensitized Oxidation and Singlet Oxygen: Consequences in Biological Systems. In:
656 Pryor, W. A. (ed.) Free Radicals in Biology. Academic Press, New York, pp 85–133.
657 doi.org/10.1016/B978-0-12-566502-5.50010-X
658
659 Frankel, E.N., 1998. Lipid Oxidation. The Oily Press, Dundee.
660
661 Frankel, E.N., Neff, W.E., Bessler, T.R., 1979. Analysis of autoxidized fats by gas
662 chromatography-mass spectrometry: V. photosensitized oxidation. Lipids 14, 961–967.
663 doi.org/10.1007/BF02533431
664
665 Galeron, M.-A., Radakovitch, O., Charrière, B., Vaultier, F., Volkman, J.K., Bianchi, T.S.,
666 Ward, N.D., Medeiros, P.M., Sawakuchi, H.O., Tank, S., Kerhervé, P., Rontani, J.-F.,

667 2018. Lipoxygenase-induced autoxidative degradation of terrestrial particulate organic
668 matter in estuaries: A widespread process enhanced at high and low latitude. Org.
669 Geochem. 115, 78–92. doi.org/10.1016/j.orggeochem.2017.10.013
670
671 Ganesh, S., Parris, D.J., Delong, E.F., Stewart, F.J., 2014. Metagenomic analysis of size-
672 fractionated picoplankton in a marine oxygen minimum zone. ISME J., 8, 187–211.
673 doi.org/10.1038/ismej.2013.144
674
675 Girotti, A.W., 1998. Lipid hydroperoxide generation, turnover, and effector action in biological
676 systems. J. Lipid Res. 39, 1529–1542.
677
678 Goad L.J., 1978. The sterols of marine Invertebrates: Composition, biosynthesis and
679 Metabolites. In Marine natural products, chemical and biologic perspectives, Vol. 2,
680 Academic Press, New York. pp. 75–172.
681
682 Grieneisen, M.L., 1994. Recent advances in our knowledge of ecdysteroid biosynthesis in
683 insects and crustaceans. Insect Biochem. Mol. Biol. 24, 115–132. doi.org/10.1016/0965-
684 1748(94)90078-7
685
686 Grossart, H.-P., Kiørboe, T., Tang, K., Ploug, H., 2003. Bacterial Colonization of Particles:
687 Growth and Interactions. Appl. Environ. Microbiol. 69, 3500–3509.
688 10.1128/AEM.69.6.3500-3509.2003
689

690 Grossart, H.-P., Tang, K.W., Kiørboe, T., Ploug, H., 2007. Comparison of cell-specific activity
691 between free-living and attached bacteria using isolates and natural assemblages. FEMS
692 Microbiol. Let. 266, 194–200. doi.org/10.1111/j.1574-6968.2006.00520.x
693
694 Guerrero, A., Casals, I., Busquets, M., Leon, Y., Manresa, A., 1997. Oxidation of oleic acid to
695 (*E*)-10-hydroperoxy-8-octadecenoic and (*E*)-10-hydroxy-8-octadecenoic acids by
696 *Pseudomonas sp.* 42A2. Biochim. Biophys. Acta 1347, 75–81. doi.org/10.1016/S0005-
697 2760(97)00056-8
698
699 Hansel, F.A., Evershed, R.P., 2009. Formation of dihydroxy acids from *Z*-monounsaturated
700 alkenoic acids and their use as biomarkers for the processing of marine commodities in
701 archaeological pottery vessels. Tetrahedron Let. 50, 5562–5564.
702 doi.org/10.1016/j.tetlet.2009.06.114
703
704 Harris, R. P., Irigoien, X., Head, R. N., Rey, C., Hygum, B. H., Hansen, B. W., Niehoff, B.,
705 Meyer-Harms, B.Carlotti, F., 2000. Feeding, growth, and reproduction in the genus
706 Calanus. ICES Journal of Marine Science, 57, 1708-1726.
707 doi.org/10.1006/jmsc.2000.0959
708
709 Harvey, H.R., Eglinton, G., O'hara, S.C.M., Corner, E.D.S., 1987. Biotransformation and
710 assimilation of dietary lipids by *Calanus* feeding on a dinoflagellate. Geochim.
711 Cosmochim. Acta 51, 3031–3040. doi.org/10.1016/0016-7037(87)90376-0
712
713 Honjo, S., Manganini, S.J., Cole, J.J., 1982. Sedimentation of biogenic matter in the deep ocean.
714 Deep Sea Res. Part A 29, 609–625. doi.org/10.1016/0198-0149(82)90079-6

Jernerèn, F., Garscha, U., Hoffmann, I., Hamberg, M., Oliw, E.H., 2010. Reaction mechanism of 5,8-linoleate diol synthase, 10*R*-dioxygenase and 8,11hydroperoxide isomerase of *Aspergillus clavatus*. Biochim. Biophys. Acta 1801, 503–507. doi.org/10.1016/j.bbalip.2009.12.012

Knox, J.P., Dodge, A.D., 1985. Singlet oxygen and plants. Phytochemistry 24, 889–896. doi.org/10.1016/S0031-9422(00)83147-7

Kokke, W.C.M.C., Bohlin, L., Fenical, W., Djerassi, C., 1982. Novel dinoflagellate 4α-methylated sterols from four Caribbean gorgonians. Phytochemistry 21, 881–887. doi.org/10.1016/0031-9422(82)80085-X

Lee, C., Wakeham, S.G., Farrington, J.W., 1983. Variations in the composition of particulate organic matter in a time-series sediment trap. Mar. Chem. 13, 181–194. doi.org/10.1016/0304-4203(83)90013-0

Léveillé, J.-C., Amblard, C., Bourdier, G., 1997. Fatty acids as specific algal markers in a natural lacustrian phytoplankton. J. Plankton Res. 19, 469–490. doi.org/10.1093/plankt/19.4.469

Li, T., Li, C., 2013. Quantitative and stereospecific dihydroxylations of Δ^5-steroids: A green synthesis of plant growth hormone intermediates. J. Agric. Food Chem. 61, 12523-12530.

739 Loidl-Stahlhofen, A., Spiteller, G., 1994. α–Hydroxyaldehydes, products of lipid peroxidation.
740 Biochim. Biophys. Acta 1211, 156-160.
741
742 Marchand, D., Rontani, J.-F., 2001. Characterisation of photooxidation and autoxidation
743 products of phytoplanktonic monounsaturated fatty acids in marine particulate matter and
744 recent sediments. Org. Geochem. 32, 287–304. doi.org/10.1016/S0146-6380(00)00175-
745 3
746
747 Martínez, E., Hamberg, M., Busquets, M., Díaz, P., Manresa, A., Oliw, E.H., 2010.
748 Biochemical characterization of the oxygenation of unsaturated fatty acids by the
749 dioxygenase and hydroperoxide isomerase of *Pseudomonas aeruginosa* 42A2. J. Biol.
750 Chem. 285, 9339–-9345. doi.org/10.1074/jbc.M109.078147
751
752 Martínez, E., Estupiñán, M., Pastor, F. I., Busquets, M., Díaz, P., Manresa, A., 2013. Functional
753 characterization of ExFadLO, an outer membrane protein required for exporting
754 oxygenated long-chain fatty acids in *Pseudomonas aeruginosa*. Biochimie 95, 290–298.
755 doi.org/10.1016/j.biochi.2012.09.032
756
757 Marty, J.-C., Zutic, V., Precali, R., Saliot, A., Cosovic, B., Smodlaka, N., Cauwet, G., 1988.
758 Organic matter characterization in the northern Adriatic Sea with special reference to the
759 sea surface microlayer. Mar. Chem. 25, 243-263.
760
761 Mayer, L.M., Schick, L.L., Hardy, K.R., Estapa, M.L., 2009. Photodissolution and other
762 photochemical changes upon irradiation of algal detritus. Limnol. Oceanogr. 54, 1688–
763 1698. doi.org/10.4319/lo.2009.54.5.1688

Mayzaud, P., Chanut, J.P., Ackman, R.G., 1989. Seasonal changes of the biochemical composition of marine particulate matter with special reference to fatty acids and sterols. Mar. Ecol. Progr. Series. 56, 189–204. doi.org/10.3354/meps056189

Merzlyak, M.N., Hendry, G.A.F., 1994. Free radical metabolism, pigment degradation and lipid peroxidation in leaves during senescence. Proc. Royal Soc. Edinburgh. Section B. 102, 459–471. doi.org/10.1017/S0269727000014482

Mize, C.E., Avigan, J., Steinberg, D., Pittman, R.C., Fales, H.M., Milne, G.W.A., 1969. A major pathway for the mammalian oxidative degradation of phytanic acid. Biochim. Biophys. Acta 176, 720–739. doi.org/10.1016/0005-2760(69)90253-7

Miralto, A., Barone, G., Romano, G., Poulet, S.A., Ianora, A., Russo, G.L., Buttino, I., Mazzarella, G., Laabir, M., Cabrini, M., Giacobbe, M.G., 1999. The insidious effect of diatoms on copepod reproduction. Nature 402, 173–176. doi.org/10.1038/46023

Monfort, P., Demers, S., Levasseur, M., 2000. Bacterial dynamics in first year sea ice and underlying seawater of Saroma-ko Lagoon (Sea of Okhotsk, Japan) and Resolute Passage (High Canadian Arctic): Inhibitory effects of ice algae on bacterial dynamics. Can. J. Microbiol. 46, 623–632. doi.org/10.1139/w00-024

Mopper, K., Zhou, J., Sri Ramana, K., Passow, U., Dam, H.G., Drapeau, D.T., 1995. The role of surface-active carbohydrates in the flocculation of a diatom bloom in a mesocosm. Deep Sea Res. Part II 42, 47–73. doi.org/10.1016/0967-0645(95)00004-A

Neff, W.E., Frankel, E.N., Fujimoto, K., 1988. Autoxidative dimerization of methyl linolenate and its monohydroperoxides, hydroperoxy epidioxides and dihydroperoxides. J. Am. Oil Chem. Soc. 65, 616–623. doi.org/10.1007/BF02540690

Nelson, J.R., 1993. Rates and possible mechanism of light-dependent degradation of pigments in detritus derived from phytoplankton. J. Mar. Res. 51, 155–179. doi.org/10.1357/0022240933223837

Nichols, P.D., Skerratt, J.H., Davidson, A., Burton, H., McMeekin, T.A., 1991. Lipids of cultured *Phaeocystis pouchetii*: Signatures for food-web, biogeochemical and environmental studies in Antarctica and the Southern ocean. Phytochemistry 30, 3209–3214. doi.org/10.1016/0031-9422(91)83177-M

Ortega-Retuerta, E., Joux, F., Jeffrey, W.H., Ghiglione, J.-F., 2013. Spatial variability of particle-attached and free-living bacterial diversity in surface waters from the Mackenzie River to the Beaufort Sea (Canadian Arctic). Biogeosciences 10, 2747–2759. doi.org/10.5194/bg-10-2747-2013

Passow, U., 2000. Formation of transparent exopolymer particles, TEP, from dissolved precursor material. Mar. Ecol. Progr. Series 192, 1–11. doi.org/10.3354/meps192001

Pedersen, L., Jensen, H.M., Burmeister, A.D., Hansen, B.W., 1999. The significance of food web structure for the condition and tracer lipid content of juvenile snail fish (Pisces:

Liparis spp.) along 65–728N off West Greenland. J. Plankt. Res. 21, 1593–1611. doi.org/10.1093/plankt/21.9.1593

Peltomaa, E., Hällfors, H., Taipale, S.J., 2019. Comparison of diatoms and dinoflagellates from different habitats as sources of PUFAs. Mar. Drugs 17, 233. doi: 10.3390/md17040233

Pohnert, G., 2000. Wound-activated chemical defense in unicellular planktonic algae. Ang. Chem. International Edition 39, 4352–4354. doi.org/10.1002/1521-3773(20001201)39:23<4352::AID-ANIE4352>3.0.CO;2-U

Pohnert, G., 2002. Phospholipase A_2 activity triggers the wound-activated chemical defence in the diatom *Thalassiosira rotula*. Plant Physiol. 129, 103–111. doi.org/10.1104/pp.010974

Porter, N.A., Mills, K.A., Carter, R.L., 1994. A mechanistic study of oleate autoxidation: competing peroxyl H-atom abstraction and rearrangement. J. Am. Chem. Soc. 116, 6690–6696. doi.org/10.1021/ja00094a026

Porter, N.A., Caldwell, S.E., Mills, K.A., 1995. Mechanisms of free radical oxidation of unsaturated lipids. Lipids 30, 277–290. doi.org/10.1007/BF02536034

Prahl, F.G., Eglinton, G., Corner, E.D.S., O'hara, S.C.M., Forsberg, T.E.V., 1984. Changes in plant lipids during passage through the gut of *Calanus*. J. Mar. Biol. Assoc. United Kingdom 64, 317–334. doi.org/10.1017/S0025315400030022

838 Rampen, S.W., Schouten, S., Abbas, B., Elda Panoto, F., Muyzer, G., Campbell, C.N., Fehling,
839 J., Sinninghe Damsté, J.S., 2007. On the origin of 24-norcholestanes and their use as age-
840 diagnostic biomarkers. Geology 35, 419–422. doi.org/10.1130/G23358A.1
841
842 Rampen, S.W., Abbas, B.A., Schouten, S., Sinninghe-Damsté, J.S.S., 2010. A comprehensive
843 study of sterols in marine diatoms (Bacillariophyta): Implications for their use as tracers
844 for diatom productivity. Limnol. Oceanogr. 55, 91–105.
845 doi.org/10.4319/lo.2010.55.1.0091
846
847 Robinson, N., Eglinton, G., Brassell, S.C., Cranwell, P.A., 1984. Dinoflagellate origin for
848 sedimentary 4α-methylsteroids and 5α(H)-stanols. Nature 308, 439–442.
849 doi.org/10.1038/308439a0
850
851 Rontani, J.-F., 2012. Photo- and free radical-mediated oxidation of lipid components during the
852 senescence of phototrophic organisms. In: Nagata, T. (Ed.), Senescence. Intech, Rijeka,
853 pp. 3–31. 10.5772/34002
854
855 Rontani, J.-F., Aubert, C., 2005. Characterization of isomeric allylic diols resulting from
856 chlorophyll phytyl side chain photo- and autoxidation by electron ionization gas
857 chromatography/mass spectrometry. Rapid Commun. Mass Spectrom. 19, 637–646.
858 doi.org/10.1002/rcm.1835
859
860 Rontani, J.-F., Volkman, J.K., 2003. Phytol degradation products as biogeochemical tracers in
861 aquatic environments. Org. Geochem. 34, 1–35. doi.org/10.1016/S0146-6380(02)00185-
862 7

Rontani, J.-F., Belt, S.T., 2020. Photo- and autoxidation of unsaturated algal lipids in the marine environment: An overview of processes, their potential tracers, and limitations. Org. Geochem. 139, 103941. doi.org/10.1016/j.orggeochem.2019.103941

Rontani, J.-F., Baillet, G., Aubert, C., 1991. Production of acyclic isoprenoid compounds during the photodegradation of chlorophyll-a in seawater. J. Photochem. Photobiol. A: Chem. 59, 369–377. doi.org/10.1016/1010-6030(91)87088-D

Rontani, J.-F., Grossi, V., Faure, F., Aubert, C., 1994. ‘‘Bound’’ 3-methylidene-7,11,15trimethylhexadecan-1,2-diol: a new isoprenoid marker for the photodegradation of chlorophyll-a in seawater. Org. Geochem. 21, 135–142. doi.org/10.1016/0146-6380(94)90150-3

Rontani, J.-F., Cuny, P., Grossi, V., 1998. Identification of a pool of lipid photoproducts in senescent phytoplanktonic cells. Org. Geochem. 29, 1215–1225. doi.org/10.1016/S0146-6380(98)00073-4

Rontani, J.-F., Bonin, P.C., Volkman, J.K., 1999. Production of Wax Esters during Aerobic Growth of Marine Bacteria on Isoprenoid Compounds. Appl. Environ. Microbiol. 65, 221–230. doi.org/10.1128/AEM.65.1.221-230.1999

Rontani, J.-F., Rabourdin, A., Marchand, D., Aubert, C., 2003. Photochemical oxidation and autoxidation of chlorophyll phytyl side chain in senescent phytoplanktonic cells: potential

sources of several acyclic isoprenoid compounds in the marine environment. Lipids 38, 241–253. doi.org/10.1007/s11745-003-1057-1

Rontani, J.-F., Charriere, B., Forest, A., Heussner, S., Vaultier, F., Petit, M., Delsaut, N., Fortier, L., Sempéré, R., 2012. Intense photooxidative degradation of planktonic and bacterial lipids in sinking particles collected with sediment traps across the Canadian Beaufort Shelf (Arctic Ocean). Biogeosciences 9, 4787–4802. doi.org/10.5194/bg-9-4787-2012

Rontani, J.-F., Belt, S. T., Vaultier, F., Brown, T. A., Massé, G., 2014. Autoxidative and photooxidative reactivity of highly branched isoprenoid (HBI) alkenes. Lipids 49, 481–494. doi.org/10.1007/s11745-014-3891-x

Rontani, J.-F., Belt, S.T., Brown, T.A., Amiraux, R., Gosselin, M., Vaultier, F., Mundy, C.J., 2016. Monitoring abiotic degradation in sinking versus suspended Arctic sea ice algae during a spring ice melt using specific lipid oxidation tracers. Org. Geochem. 98, 82–97. doi.org/10.1016/j.orggeochem.2016.05.016

Rontani, J.-F., Amiraux, R., Lalande, C., Babin, M., Kim, H.-R., Belt, S.T., 2018. Use of palmitoleic acid and its oxidation products for monitoring the degradation of ice algae in Arctic waters and bottom sediments. Org. Geochem. 124, 88–102. doi.org/10.1016/j.orggeochem.2018.06.002

911 Schaich, K.M., 2005. Lipid oxidation: theoretical aspects. In: Shahidi, F. (Ed.), Bailey's
912 Industrial Oil and Fat Products. John Wiley & Sons, Chichester, pp. 269–355.
913 10.1002/047167849X.bio067
914
915 Sheldon, R.A., Kochi, J.K., 1976. Metal-catalyzed oxidations of organic compounds in the
916 liquid phase. A mechanistic approach. Adv. Catalys. 25, 272–413.
917 doi.org/10.1016/S0360-0564(08)60316-8
918
919 Sheridan, C.C., Lee, C., Wakeham, S.G., Bishop, J.K.B., 2002. Suspended particle organic
920 composition and cycling in surface and midwaters of the EqPac Ocean. Deep-Sea Res. I
921 49, 1983–2008, doi:10.1016/S0967-0637(02)00118-8
922
923 Shimizu, Y., Alam, M.Kobayashi, A., 1976. Dinosterol, the major sterol with a unique side
924 chain in the toxic dinoflagellate, *Gonyaulax tamarensis*. J. Am. Chem. Soc. 98, 1059–
925 1060. doi.org/10.1021/ja00420a054
926
927 Shoja Chaghervand, S., 2019. Characterization of the enzymes involved in the diolsynthase
928 pathway in *Pseudomonas aeruginosa* (PhD Thesis). Universitat de Barcelona. Spain
929
930 Suh, M.J., Baek, K.Y., Kim, B.S., Hou, C.T., Kim, H.R., 2011. Production of 7,10-dihydroxy-
931 8(*E*)-octadecenoic acid from olive oil by *Pseudomonas aeruginos*a PR3. Appl. Microbiol.
932 Biotechnol. 89, 1721–1727.
933

Sun, M.-Y., Aller, R.C., Lee, C., Wakeham, S.G., 2002. Effects of oxygen and redox oscillation on degradation of cell-associated lipids in surficial marine sediments. Geochim. Cosmochim. Acta 66, 2003–2012.

Suzuki, N., Yasuo, N., Nakajo, T., and Shine, H., 2005. Possible origin of 24-norcholesterol in marine environment. Org. Geochem. Challenges for the 21st Century. 22 IMOG Seville, Spain, Abstract OB2-2.

Taipale, S. J., Hiltunen, M., Vuorio, K.Peltomaa, E., 2016. Suitability of phytosterols alongside fatty acids as chemotaxonomic biomarkers for phytoplankton. Front. Plant Sci. 7, 212. doi.org/10.3389/fpls.2016.00212

Tanoue, E., Handa, N., 1980. Vertical transport of organic materials in the northern North Pacific as determined by sediment trap experiment. J. Oceanogr. Soc. Japan 36, 231–245. doi.org/10.1007/BF02072124

Tarran, G.A., Bruun, J.T., 2015. Nanoplankton and picoplankton in the Western English Channel: abundance and seasonality from 2007–2013. Progr. Oceanogr. 137, 446–455. doi.org/10.1016/j.pocean.2015.04.024

Véron, B., Dauguet, J.-C., Billard, C., 1998. Sterolic biomarkers in marine phytoplankton. II. Free and conjugated sterols of seven species used in mariculture. J. Phycol. 34, 273–279. doi.org/10.1046/j.1529-8817.1998.340273.x

Volkman, J.K., 1986. A review of sterol markers for marine and terrigenous organic matter. Org. Geochem. 9, 83–99. doi.org/10.1016/0146-6380(86)90089-6

Volkman, J.K., 2003. Sterols in microorganisms. Appl. Microbiol. Biotechnol. 60, 495–506. doi.org/10.1007/s00253-002-1172-8

Wakeham, S.G., Farrington, J.W., Gagosian, R.B., 1985. Variability in lipid flux and composition of particulate matter in the Peru upwelling region. Org. Geochem. 6, 203–215. doi.org/10.1016/0146-6380(84)90042-1

Wakeham, S.G., Canuel, E., 1988. Organic geochemistry of particulate matter in the eastern tropical North Pacific Ocean: Implications for particle dynamics. J. Mar. Res. 46, 183–213. doi.org/10.1357/002224088785113748

Wakeham, S.G., Lee, C., 1989. Organic geochemistry of particulate matter in the ocean: The role of particles in oceanic sedimentary cycles. Org. Geochem. 14, 83–96, doi:10.1016/0146-6380(89)90022-3

Widdicombe, C.E., Eloire, D., Harbour, D., Harris, R.P., Somerfield, P.J., 2010. Long-term phytoplankton community dynamics in the Western English Channel. J. Plankt. Res. 32, 643–655. doi.org/10.1093/plankt/fbp127

Wood, B.J.B., 1974. Fatty acids and saponifiable lipids. In: Steward, W.D. (Ed.), Algal Physiology and Biochemistry. University of California Press, Berkeley, pp. 236-265.

983

984 Zafiriou, O.C., Joussot-Dubien, J., Zepp, R.G., Zika, R.G., 1984. Photochemistry of natural

985 waters. Environ. Sci. Technol. 18, 358A–371A. doi.org/10.1021/es00130a711

986

987

FIGURE CAPTIONS

Figure 1. Map of the study area with location of the L4 station investigated.

Figure 2. Time series of sterol concentrations in SPM samples collected at 5 m (A) and 25 m (B) from January to December 2018 at the L4 station.

Figure 3. Time series of acyclic isoprenoid acid concentrations in SPM samples collected at 5 m (A) and 25 m (B) from January to December 2018 at the L4 station.

Figure 4. Time series of the proportion of the main classes of fatty acids (SFAs, MUFAs and PUFAs) (A), phytol (**12**) concentration (µg L^{-1}) (B) and chlorophyll photooxidation estimate (%) (C) in SPM samples collected at 5 m from January to December 2018 at the L4 station.

Figure 5. Time series of biotic and abiotic degradation percentage of palmitoleic acid (**22**) in SPM samples collected at 5 m (A) and 25 m (B) from January to December 2018 and at 25 m from January to December 2019 (C) at the L4 station.

Figure 6. Partial ion chromatograms (*m/z* 199.1518, 213.1675, 329.1968 and 343.2125) showing the presence of palmitoleic acid (**22**) oxidation products in silylated TLEs in SPM samples collected at 5 m (A) and 25 m (B) on 04/30/18 at the L4 station.

Figure 7. Formation and degradation pathways of 10*S*-hydroperoxyhexadec-8(*E*)-enoic acid (**30**).

Figure 8. Conceptual scheme showing the defense system of diatoms during copepod grazing and the involvement of FFA detoxification in associated bacteria. (PUA = polyunsaturated aldehydes, 7,10-DS = 7,10-diol synthase, 10*S*-DOX = 10*S*-dioxygenase, 10*S*-HPHA = 10*S*-hydroperoxyhexadecen-8(*E*)-enoic acid, 7,10-DiOHHA = 7,10-dihydroxyhexadecen-8(*E*)-enoic acid).

Supplementary material

Figure S1. Partial ion chromatograms (*m/z* 225.1670, 315.2171, 327.1807 and 417.2808) of silylated TLE of the SPM sample collected on 04/30/18 at 25 m (A) and standard *threo* 7,10-dihydroxyhexadec-8(*E*)-enoic acid (**42**) TMS derivative (B).

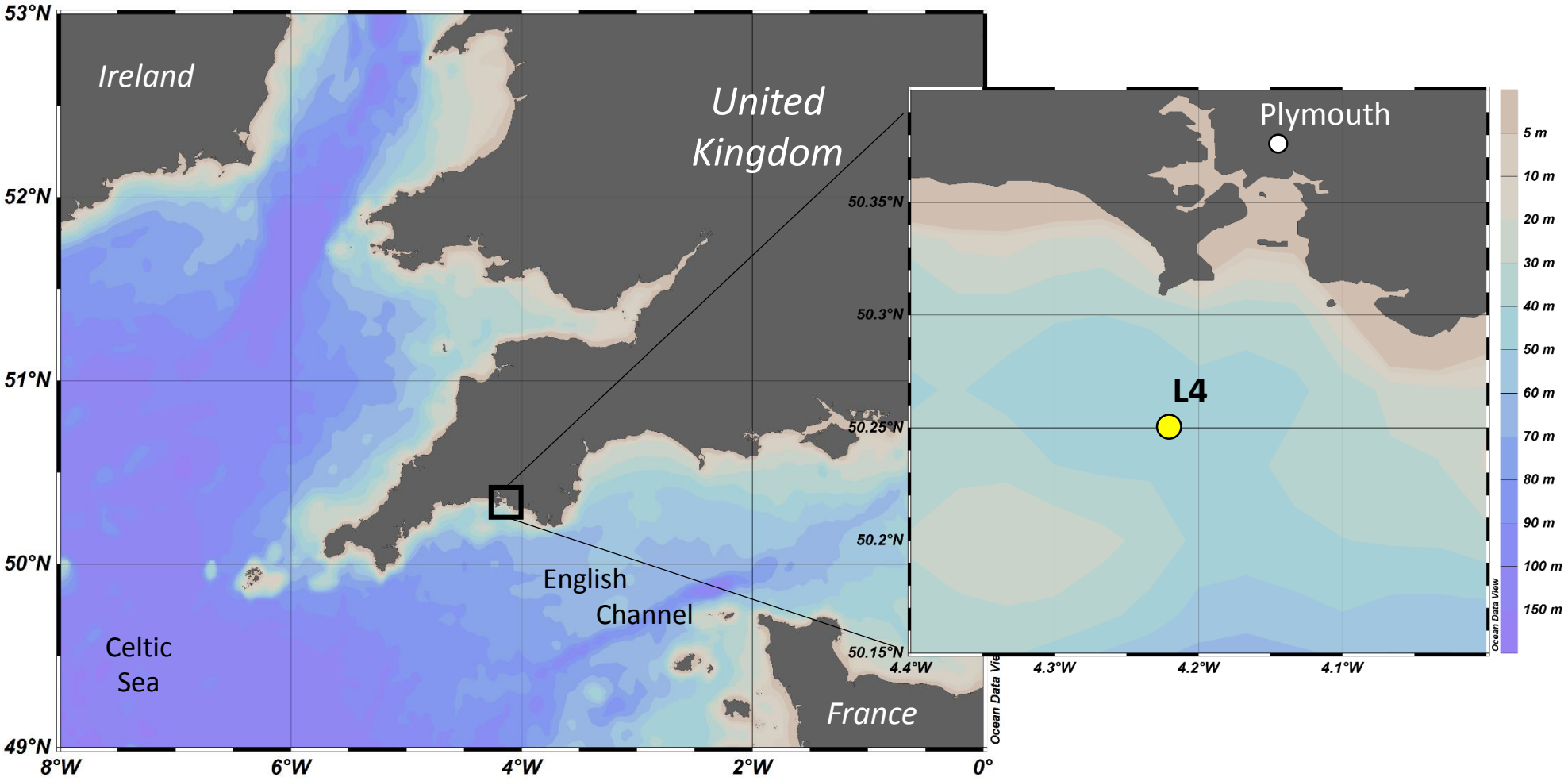
Ireland
United Kingdom
Celtic Sea
English Channel
France
Plymouth
L4
53°N
52°N
51°N
50°N
49°N
8°W
6°W
4°W
2°W
0°
50.35°N
50.3°N
50.25°N
50.2°N
50.15°N
4.4°W
4.3°W
4.2°W
4.1°W
5 m
10 m
20 m
30 m
40 m
50 m
60 m
70 m
80 m
90 m
100 m
150 m
Ocean Data View

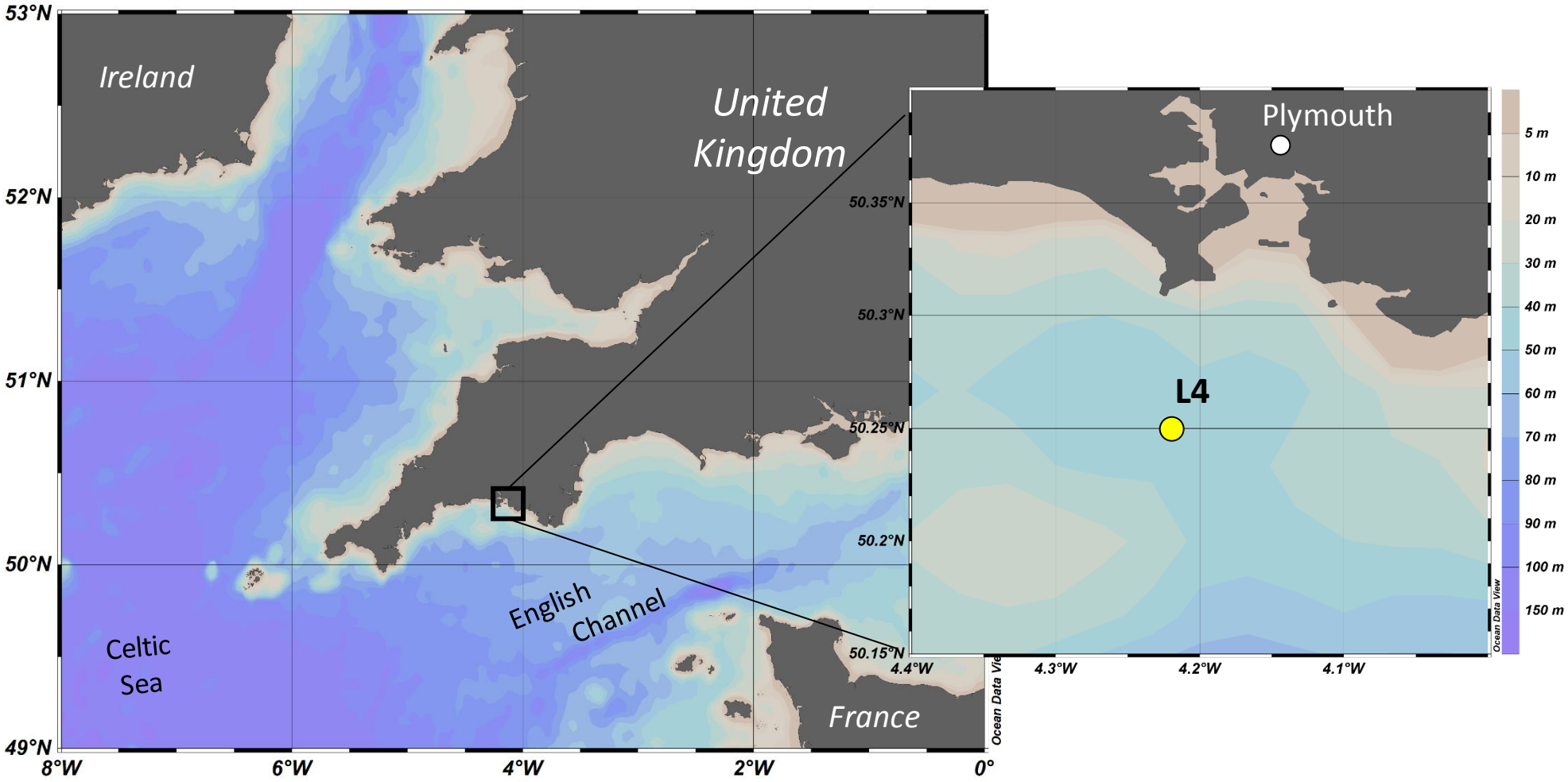
Ireland
United Kingdom
Celtic Sea
English Channel
France
Plymouth
L4
53°N
52°N
51°N
50°N
49°N
8°W
6°W
4°W
2°W
0°
50.35°N
50.3°N
50.25°N
50.2°N
50.15°N
4.4°W
4.3°W
4.2°W
4.1°W
5 m
10 m
20 m
30 m
40 m
50 m
60 m
70 m
80 m
90 m
100 m
150 m
Ocean Data View

5 m

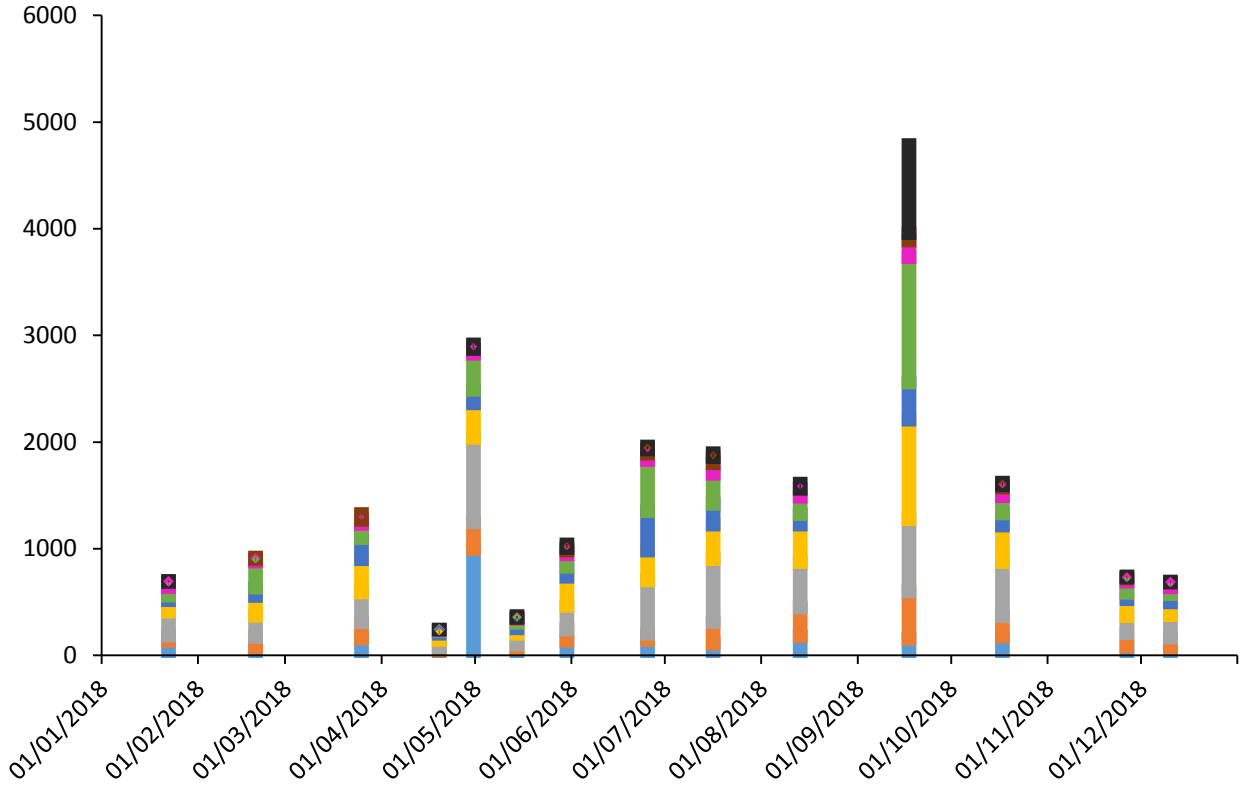
6000
5000
4000
3000
2000
1000
0
01/01/2018
01/02/2018
01/03/2018
01/04/2018
01/05/2018
01/06/2018
01/07/2018
01/08/2018
01/09/2018
01/10/2018
01/11/2018
01/12/2018

25 m

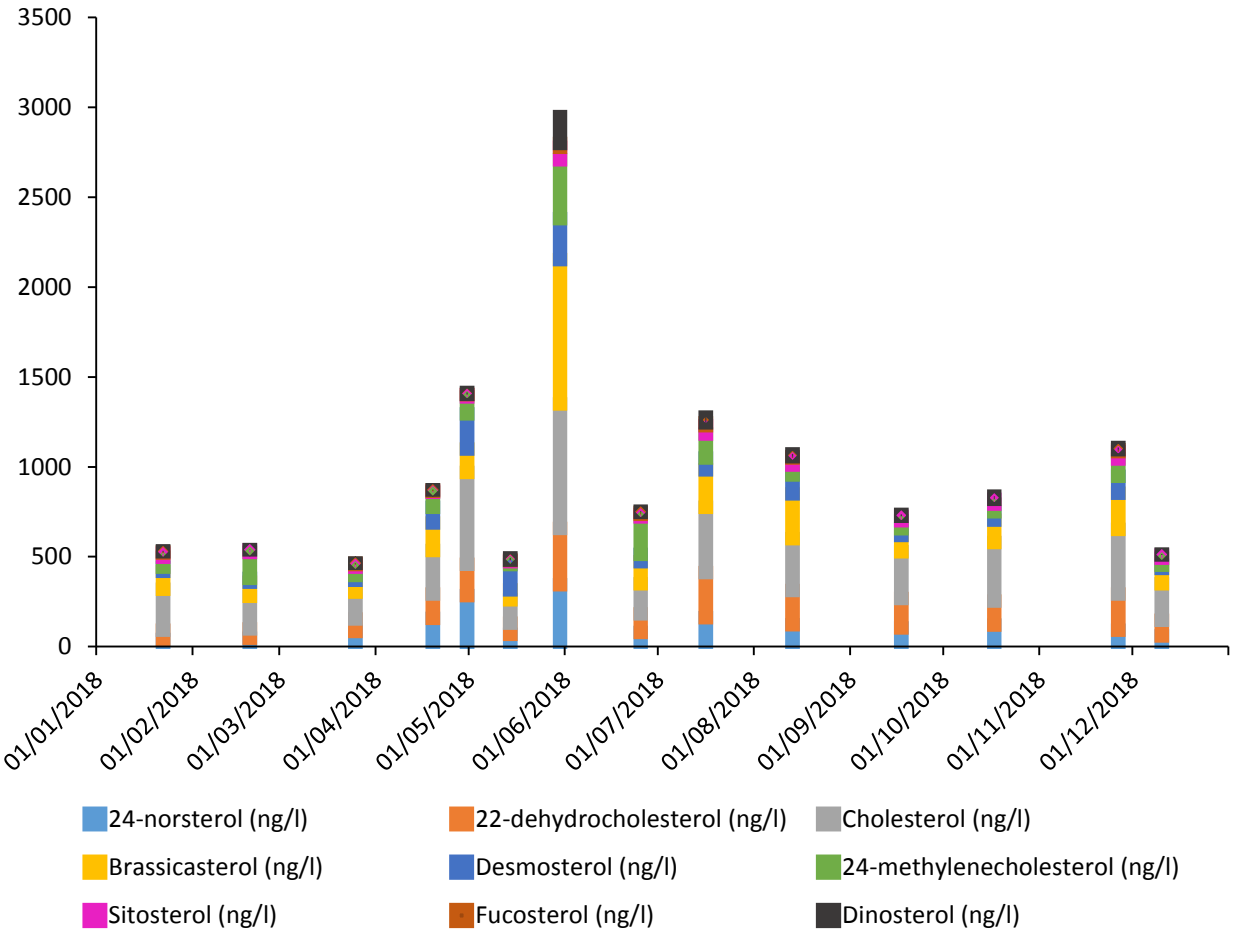
3500
3000
2500
2000
1500
1000
500
0
01/01/2018
01/02/2018
01/03/2018
01/04/2018
01/05/2018
01/06/2018
01/07/2018
01/08/2018
01/09/2018
01/10/2018
01/11/2018
01/12/2018
24-norsterol (ng/l)
22-dehydrocholesterol (ng/l)
Cholesterol (ng/l)
Brassicasterol (ng/l)
Desmosterol (ng/l)
24-methylenecholesterol (ng/l)
Sitosterol (ng/l)
Fucosterol (ng/l)
Dinosterol (ng/l)

5 m

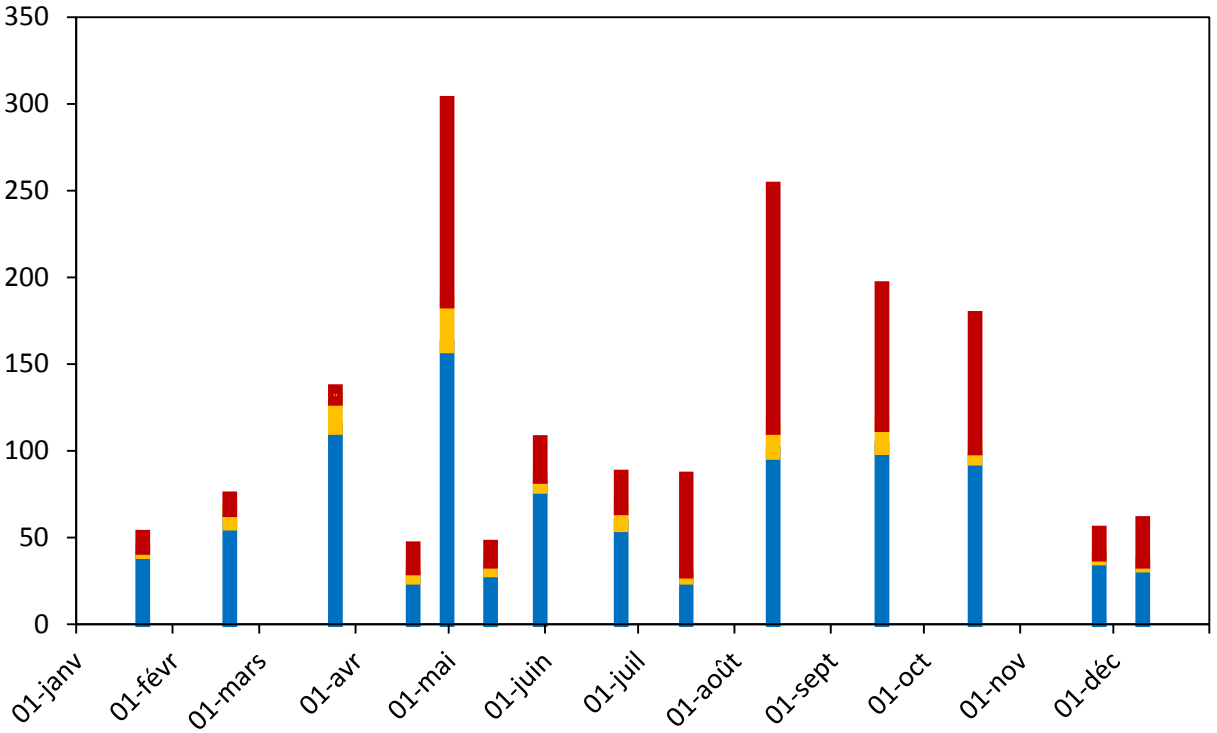
350
300
250
200
150
100
50
0
01-janv
01-févr
01-mars
01-avr
01-mai
01-juin
01-juil
01-août
01-sept
01-oct
01-nov
01-déc

25 m

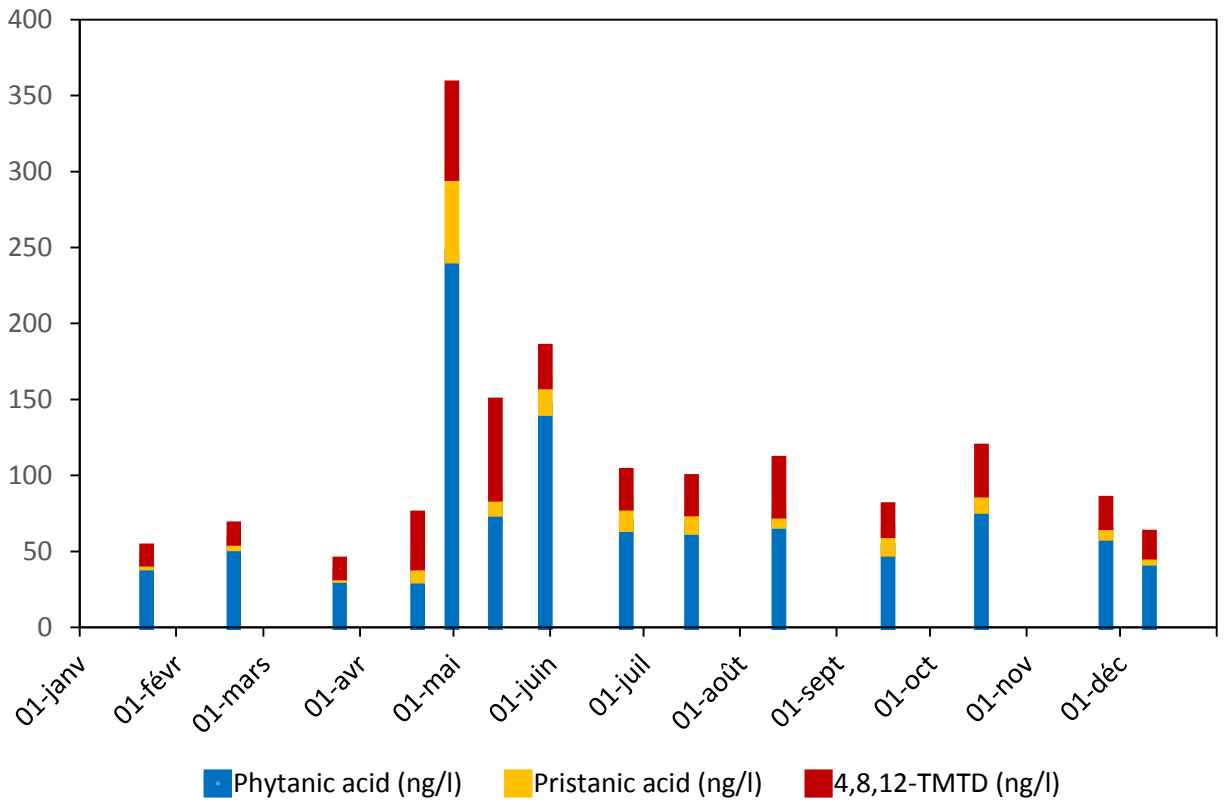
400
350
300
250
200
150
100
50
0
01-janv
01-févr
01-mars
01-avr
01-mai
01-juin
01-juil
01-août
01-sept
01-oct
01-nov
01-déc
Phytanic acid (ng/l)
Pristanic acid (ng/l)
4,8,12-TMTD (ng/l)

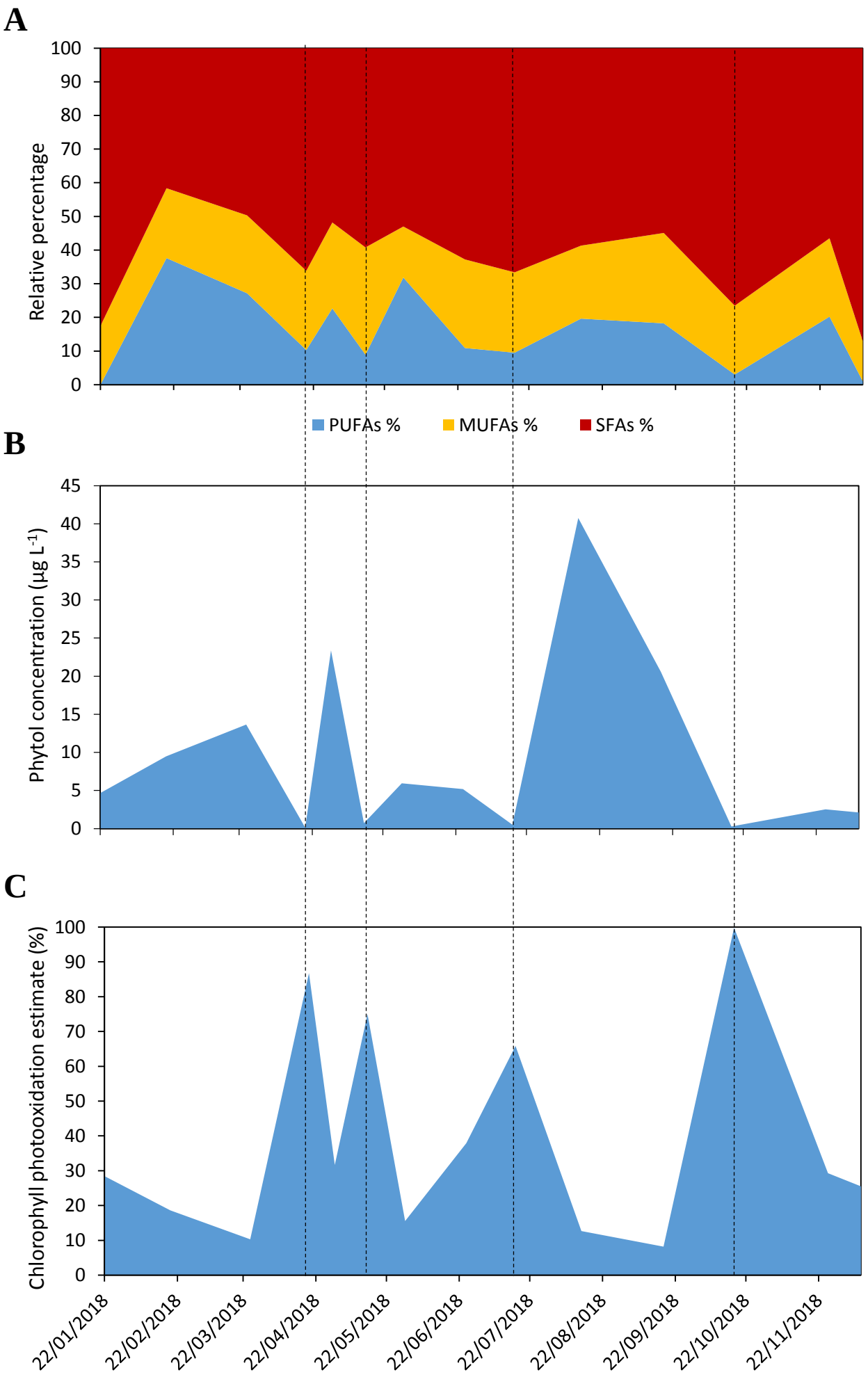
A
Relative percentage
100
90
80
70
60
50
40
30
20
10
0
PUFAs %
MUFAs %
SFAs %
B
Phytol concentration (µg L-1)
45
40
35
30
25
20
15
10
5
0
C
Chlorophyll photooxidation estimate (%)
100
90
80
70
60
50
40
30
20
10
0
22/01/2018
22/02/2018
22/03/2018
22/04/2018
22/05/2018
22/06/2018
22/07/2018
22/08/2018
22/09/2018
22/10/2018
22/11/2018

5 m

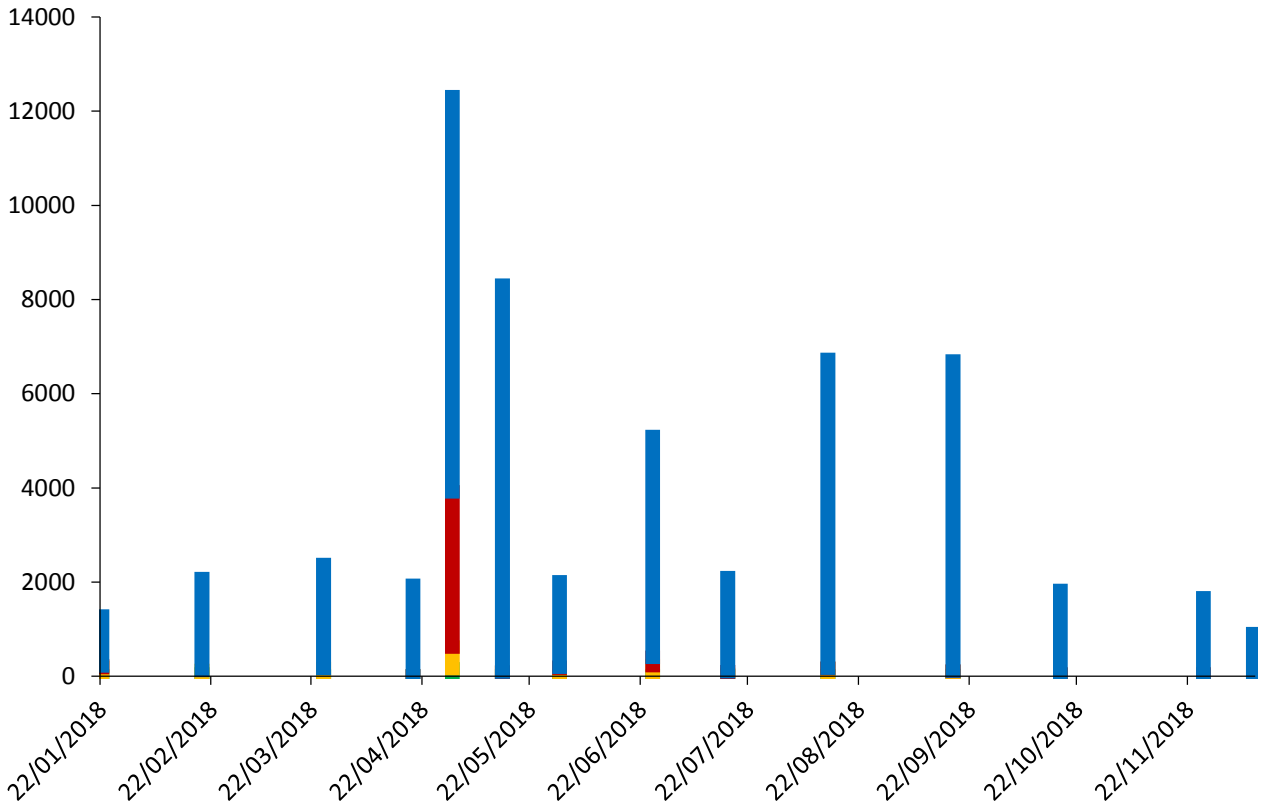
14000
12000
10000
8000
6000
4000
2000
0
22/01/2018
22/02/2018
22/03/2018
22/04/2018
22/05/2018
22/06/2018
22/07/2018
22/08/2018
22/09/2018
22/10/2018
22/11/2018

25 m

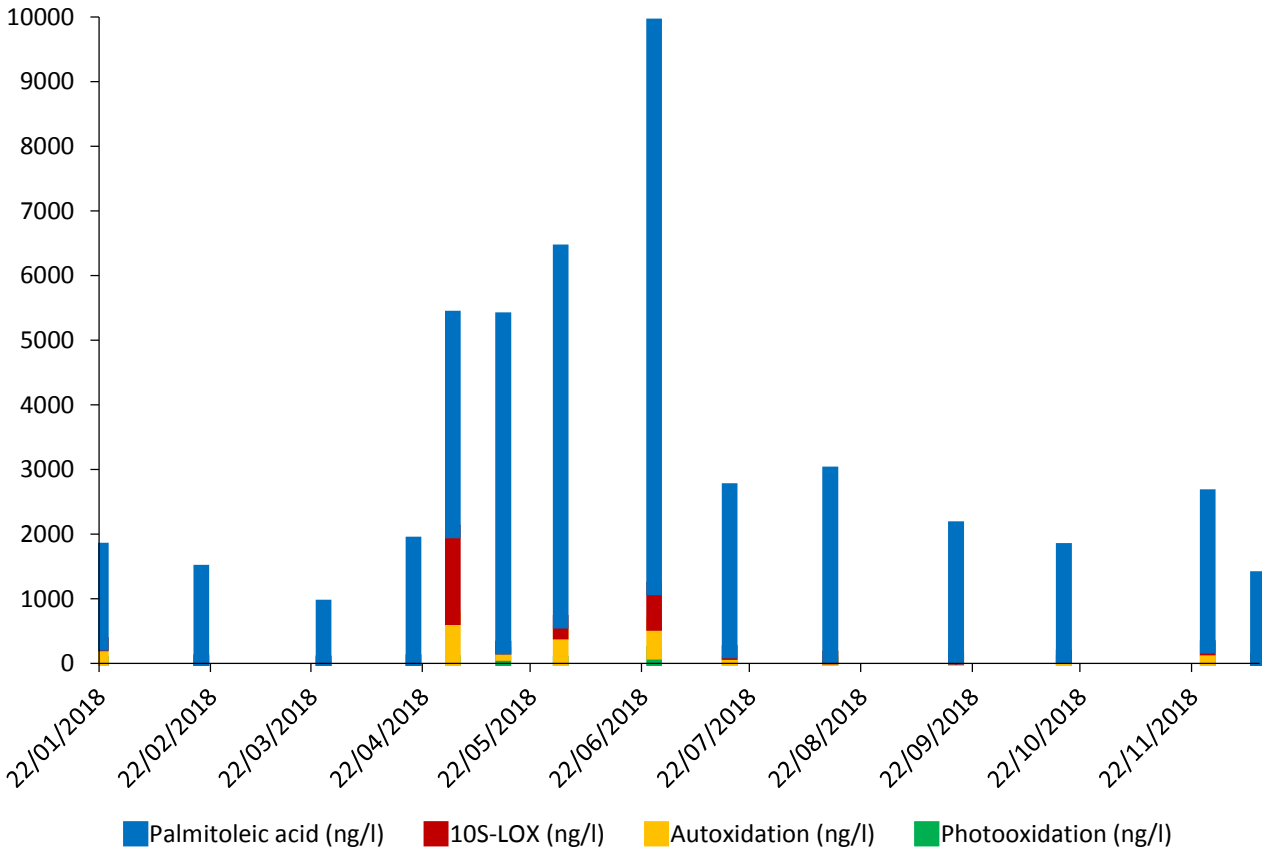
10000
9000
8000
7000
6000
5000
4000
3000
2000
1000
0
22/01/2018
22/02/2018
22/03/2018
22/04/2018
22/05/2018
22/06/2018
22/07/2018
22/08/2018
22/09/2018
22/10/2018
22/11/2018
Palmitoleic acid (ng/l)
10S-LOX (ng/l)
Autoxidation (ng/l)
Photooxidation (ng/l)

A

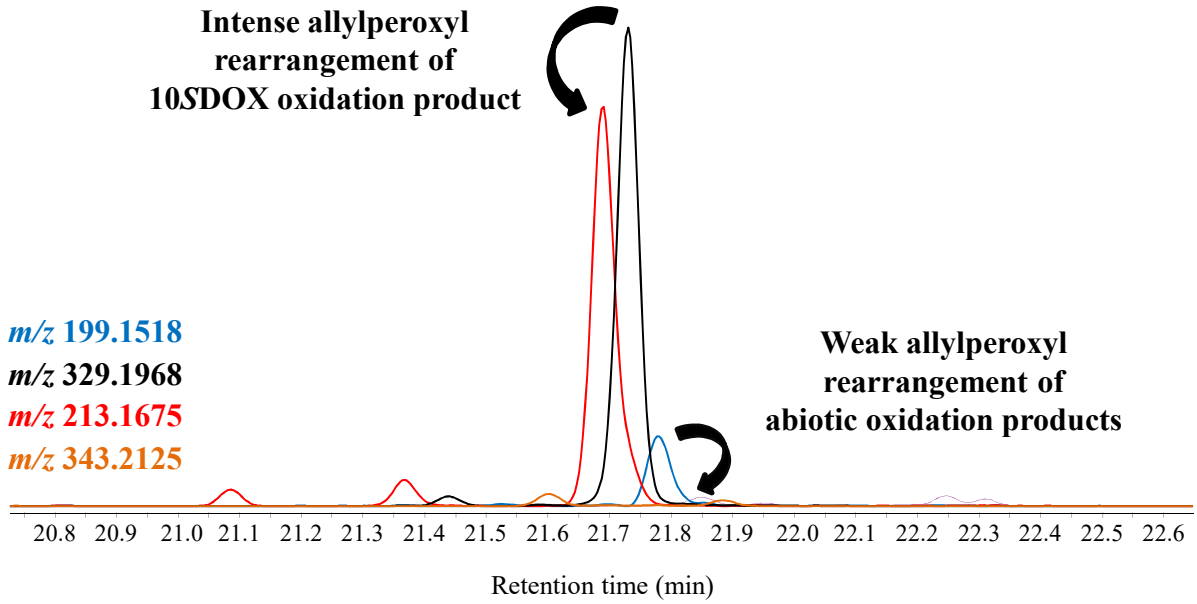
Intense allylperoxyl rearrangement of 10SDOX oxidation product
m/z 199.1518
m/z 329.1968
m/z 213.1675
m/z 343.2125
Weak allylperoxyl rearrangement of abiotic oxidation products
20.8 20.9 21.0 21.1 21.2 21.3 21.4 21.5 21.6 21.7 21.8 21.9 22.0 22.1 22.2 22.3 22.4 22.5 22.6
Retention time (min)

B

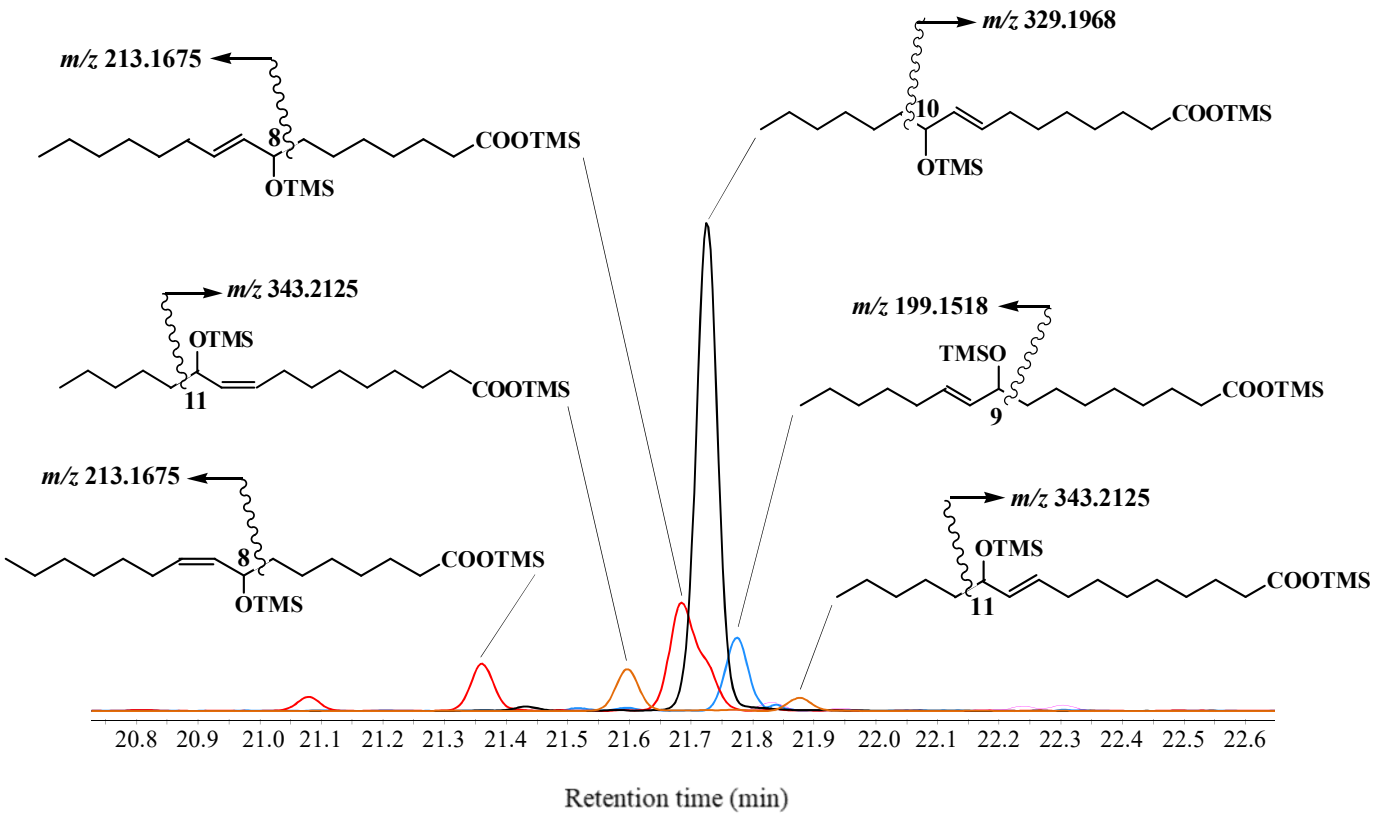
m/z 213.1675
8
COOTMS
OTMS
m/z 329.1968
10
COOTMS
OTMS
m/z 343.2125
OTMS
11
COOTMS
m/z 199.1518
TMSO
9
COOTMS
m/z 213.1675
8
COOTMS
OTMS
m/z 343.2125
OTMS
11
COOTMS
20.8 20.9 21.0 21.1 21.2 21.3 21.4 21.5 21.6 21.7 21.8 21.9 22.0 22.1 22.2 22.3 22.4 22.5 22.6
Retention time (min)

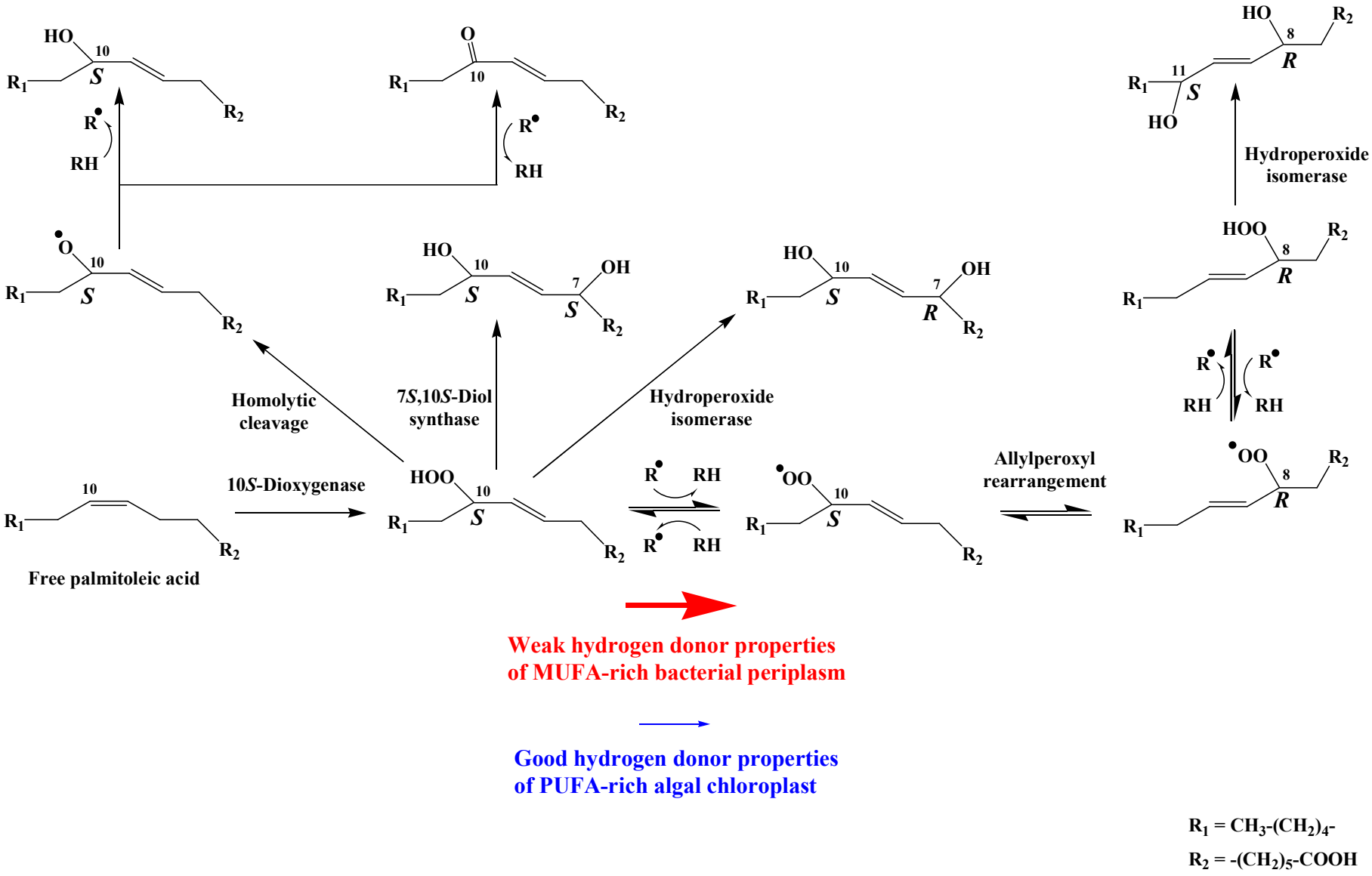
Free palmitoleic acid
10S-Dioxygenase
Homolytic cleavage
7S,10S-Diol synthase
Hydroperoxide isomerase
Allylperoxyl rearrangement
Hydroperoxide isomerase
Weak hydrogen donor properties of MUFA-rich bacterial periplasm
Good hydrogen donor properties of PUFA-rich algal chloroplast
R1 = CH3-(CH2)4-
R2 = -(CH2)5-COOH

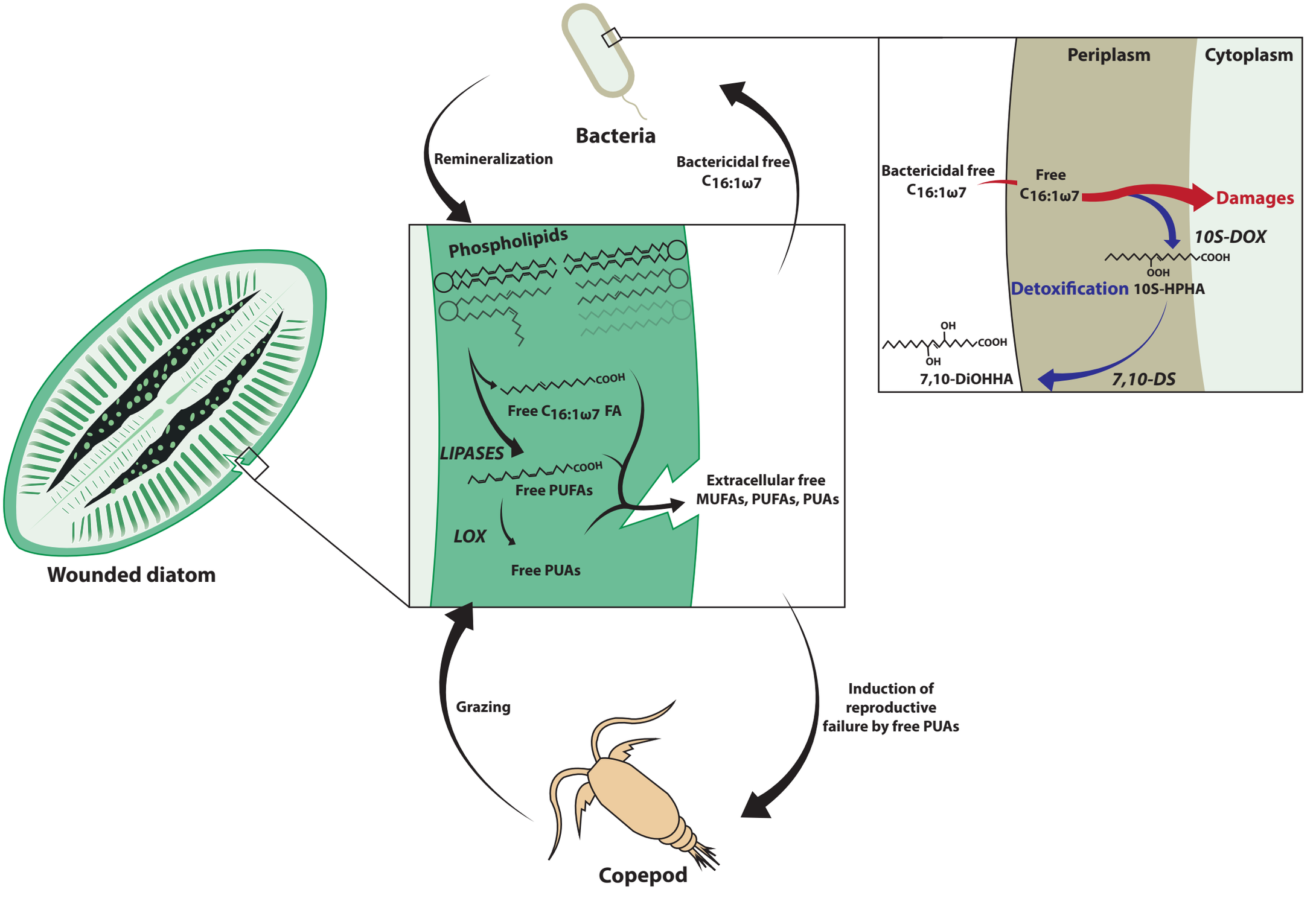
Bacteria
Remineralization
Bactericidal free
C16:1ω7
Phospholipids
COOH
Free C16:1ω7 FA
LIPASES
COOH
Free PUFAs
LOX
Free PUAs
Extracellular free
MUFAs, PUFAs, PUAs
Wounded diatom
Periplasm
Cytoplasm
Bactericidal free
C16:1ω7
Free
C16:1ω7
Damages
10S-DOX
COOH
OOH
Detoxification 10S-HPHA
OH
COOH
OH
7,10-DiOHHA
7,10-DS
Grazing
Induction of
reproductive
failure by free PUAs
Copepod

Table 1. Concentrations of sterols and acyclic isoprenoid compounds and chlorophyll photooxidation estimates in spm samples collected at station L4 during the time series 2018 at 5 m.

	01/25	02/18	03/25	04/19	04/30	05/14	05/30	06/25	07/16	08/13	09/17	10/17	11/26	12/10
24-Norcholesta-5,22*E*-dien-3β-ol (24-norsterol)[a]	137.1	74.9	156.4	45.8	996.0	62.2	136.9	143.4	109.0	178.6	155.3	174.6	81.5	68.9
Cholesta-5,22*E*-dien-3β-ol (22-dehydrocholesterol)[a]	46.9	98.1	152.4	29.4	249.5	40.9	103.7	58.6	203.8	269.1	442.3	192.8	127.8	96.9
Cholest-5-en-3β-ol (cholesterol)[a]	224.6	196.1	279.4	70.6	791.9	97.9	221.1	500.7	588.9	426.3	679.3	506.5	157.8	211.3
24-Methylcholesta-5,22*E*-dien-3β-ol (brassicasterol)[a]	109.2	185.8	312.3	55.9	323.7	51.7	273.6	278.8	323.0	349.3	932.4	340.7	158.1	119.7
Cholest-5,24-dien-3β-ol (desmosterol)[a]	41.3	77.6	198.7	27.4	128.1	50.8	92.1	368.4	196.2	99.6	348.7	116.0	61.8	79.3
24-Methylcholesta-5,24(28)-dien-3β-ol (24-methylenecholesterol)[a]	80.2	248.6	132.2	7.9	336.5	38.7	119.0	479.8	281.4	163.5	1173.6	159.9	103.0	60.7
24-Ethylcholest-5-en-3β-ol (sitosterol)[a]	48.5	23.1	39.6	4.1	47.2	5.6	36.9	60.6	97.8	74.3	156.6	82.7	31.1	45.2
24-Ethylcholesta-5,22*E*-dien-3β-ol (fucosterol)[a]	nd[e]	13.8	55.5	nd	nd	5.0	23.2	38.3	57.1	nd	71.0	19.3	8.2	nd
4α,23,24-Trimethyl-5α-cholest-22*E*-en-3-ol (dinosterol)[a]	10.7	nd	nd	1.2	42.8	17.9	35.0	30.3	38.3	52.0	827.0	29.1	12.1	12.2
Total sterols[a]	698.6	917.9	1326.6	242.2	2215.7	370.7	1041.4	1958.9	1895.6	1612.7	4786.2	1621.6	741.2	693.3
Phytol[b]	4.67	9.47	13.65	0.13	23.37	0.72	5.93	5.17	0.52	40.75	20.57	0.28	2.54	2.13
Phytyldiol[b]	0.11	0.13	0.10	0.02	0.60	0.07	0.07	0.17	0.04	0.37	0.12	0.14	0.06	0.04
Phytanic acid[a]	41.6	58.0	113.1	26.8	160.1	31.1	79.2	57.1	26.8	98.8	101.5	95.3	37.8	33.7
Pristanic acid[a]	2.3	7.7	16.7	5.4	25.9	5.1	5.8	9.8	3.6	14.3	13.1	6.0	2.2	2.3
4,8,12-TMTD acid[a]	5.5	46.2	82.2	11.7	16.1	9.0	10.4	7.5	4.5	19.6	23.8	20.0	6.9	7.1
CPPI[c]	0.018	0.011	0.006	0.115	0.021	0.078	0.009	0.026	0.060	0.007	0.005	0.392	0.019	0.016
Chlorophyll photooxidation estimate (%)[d]	28.5	18.6	10.3	86.7	31.7	75.0	15.5	37.9	65.3	12.7	8.2	99.8	29.3	25.5

[a] (ng L^{-1})
[b] (µg L^{-1})
[c] Chlorophyll Phytyl side-chain Photooxidation Index (molar ratio phytyldiol/phytol).
[d] Estimated with the empirical equation: chlorophyll photodegradation % = $(1 - [CPPI + 1]^{-18.5}) \times 100$ (Cuny et al. 2002).
[e] Not detected

Table 2. Concentrations of sterols and acyclic isoprenoid compounds and chlorophyll photooxidation estimates in spm samples collected at station L4 during the time series 2018 at 25 m.

	01/25	02/18	03/25	04/19	04/30	05/14	05/30	06/25	07/16	08/13	09/17	10/17	11/26	12/10
24-Norcholesta-5,22*E*-dien-3β-ol (24-norsterol)[a]	38.6	46.2	84.6	88.2	284.1	67.4	344.5	79.2	160.6	120.7	104.1	120.0	90.6	58.4
Cholesta-5,22*E*-dien-3β-ol (22-dehydrocholesterol)[a]	51.9	51.7	69.1	82.0	173.5	62.7	312.2	102.1	251.3	190.5	161.8	132.7	200.8	87.9
Cholest-5-en-3β-ol (cholesterol)[a]	227.7	182.0	150.0	171.4	511.0	131.0	692.3	168.5	362.4	288.9	259.4	325.4	360.6	203.2
24-Methylcholesta-5,22*E*-dien-3β-ol (brassicasterol)[a]	100.0	78.2	65.8	70.2	130.2	53.5	803.2	121.5	208.7	249.9	91.1	125.0	201.0	84.8
Cholest-5,24-dien-3β-ol (desmosterol)[a]	23.6	20.8	25.2	184.3	195.6	140.8	227.5	40.9	66.2	106.5	36.8	45.1	94.9	18.3
24-Methylcholesta-5,24(28)-dien-3β-ol (24-methylenecholesterol)[a]	55.5	145.2	47.4	217.7	95.5	16.6	328.6	207.9	133.3	54.5	45.2	42.6	95.3	38.6
24-Ethylcholest-5-en-3β-ol (sitosterol)[a]	22.0	14.2	14.6	10.2	11.9	7.8	69.2	15.3	46.4	39.6	24.0	27.1	42.2	19.0
24-Ethylcholesta-5,22*E*-dien-3β-ol (fucosterol)[a]	7.3	nd[e]	5.7	2.4	2.1	1.8	20.1	9.6	16.3	6.4	nd	nd	9.3	nd
4α,23,24-Trimethyl-5α-cholest-22*E*-en-3-ol (dinosterol)[a]	5.2	1.4	3.0	1.3	9.5	12.1	150.1	7.6	31.4	16.4	11.8	13.0	12.8	5.3
Total sterols[a]	545.0	539.7	465.4	871.5	1414.9	493.8	2948.8	753.5	1276.7	1072.4	735.9	836.8	1114.7	515.5
Phytol[b]	8.53	8.38	2.83	2.82	12.40	14.20	42.17	26.92	11.97	16.03	6.44	7.21	14.75	6.85
Phytyldiol[b]	0.06	0.12	0.06	0.04	0.16	0.18	0.34	0.48	0.16	0.12	0.08	0.14	0.10	0.10
Phytanic acid[a]	41.9	54.6	33.8	33.4	243.9	77.3	143.6	67.1	65.4	69.4	50.9	79.2	61.6	45.2
Pristanic acid[a]	2.5	3.5	1.5	8.6	54.4	10.1	17.6	14.1	12.2	6.6	12.2	10.8	6.8	4.0
4,8,12-TMTD acid[a]	6.5	7.3	6.9	30.5	55.3	60.1	21.0	19.2	18.9	32.5	14.9	26.6	13.8	10.8
CPPI (%)[c]	0.006	0.012	0.016	0.011	0.011	0.010	0.016	0.014	0.011	0.006	0.010	0.016	0.005	0.012
Chlorophyll photooxidation estimate (%)[d]	10.4	19.6	26.0	17.8	17.8	16.9	11.8	23.3	18.2	10.2	16.7	25.0	9.6	20.0

[a] (ng L^{-1})
[b] (µg L^{-1})
[c] Chlorophyll Phytyl side-chain Photooxidation Index (molar ratio phytyldiol/phytol).
[d] Estimated with the empirical equation: chlorophyll photodegradation % = $(1 - [CPPI + 1]^{-18.5}) \times 100$ (Cuny et al. 2002).
[e] Not detected

Table 3. Fatty acid concentrations (µg L^{-1}) in spm samples collected at station L4 during the time series 2018 at 5 m.

	01/25	02/18	03/25	04/19	04/30	05/14	05/30	06/25	07/16	08/13	09/17	10/17	11/26	12/10
$C_{12:0}$	0.16	0.08	0.18	0.24	0.31	0.24	0.24	0.55	0.17	0.29	0.43	0.36	0.13	0.11
$C_{14:0}$	1.38	1.87	2.49	3.54	6.83	6.08	4.09	5.72	2.15	14.71	5.56	2.92	1.65	1.39
$BrC_{15:0}$	0.20	0.20	0.44	0.63	0.54	0.52	0.71	0.60	0.38	1.32	1.66	0.58	0.21	0.26
$C_{15:0}$	0.46	0.44	0.81	0.48	1.40	0.75	1.13	1.09	0.54	0.76	0.84	1.20	0.29	0.69
$C_{16:4}$	nd[a]	0.86	0.53	nd	1.36	nd	2.29	nd	nd	3.77	0.52	nd	0.30	nd
$C_{16:1\omega7}$	1.06	1.95	2.80	2.15	8.39	9.03	1.82	4.69	1.99	6.56	6.58	1.78	1.62	0.90
$C_{16:0}$	4.80	4.17	6.95	9.27	11.18	15.88	9.33	10.23	6.58	25.69	16.72	9.19	3.35	6.97
$C_{18:4}$	nd	1.94	3.40	1.53	2.24	1.82	2.24	0.86	0.35	2.14	2.59	0.67	0.84	0.18
$C_{18:1\omega9}$	0.84	1.78	3.04	2.25	2.62	3.70	2.66	3.16	1.14	8.10	3.15	2.13	0.79	0.79
$C_{18:1\omega7}$	0.23	0.45	0.97	1.23	0.73	1.00	0.60	0.82	1.15	2.49	4.07	0.61	0.31	0.34
$C_{18:0}$	3.10	1.58	2.46	1.69	3.53	2.03	2.22	2.51	2.08	3.63	3.00	2.70	0.99	5.38
$C_{20:5}$	nd	3.68	1.91	0.94	4.34	2.02	2.34	1.54	0.75	2.20	1.88	nd	0.78	nd
$C_{22:6}$	nd	1.07	1.44	nd	2.46	nd	3.78	1.20	0.60	7.39	4.37	nd	0.45	nd
Total fatty acids	12.20	20.07	26.81	23.96	45.93	43.07	33.45	32.94	17.87	79.05	51.40	22.12	11.69	17.00
SFAs (%)	82.6	41.6	49.7	66.2	51.8	59.2	53.0	62.8	66.6	58.7	54.9	76.5	56.5	87.0
MUFAs (%)	17.4	20.8	23.1	23.5	25.6	31.9	15.2	26.3	23.9	21.7	26.9	20.4	23.3	11.9
PUFAs (%)	nd	37.6	21.2	10.3	22.8	8.9	31.8	10.9	9.5	19.6	12.2	3.1	20.2	1.1
Diatom fatty acid ratio[b]	0.5	1.1	0.8	0.6	1.5	1.0	0.9	1.0	0.6	1.0	0.8	0.5	1.1	0.3
(MUFAs+PUFAs)/SFAs	0.2	1.4	1.0	0.5	0.9	0.7	0.9	0.6	0.5	0.7	0.8	0.3	0.8	0.2

[a] Not detected

[b] $(C_{14:0} + C_{16:1\omega7} + \Sigma C_{16}$ PUFAs$)/C_{16:0}$

[c] (Σ *iso* and *anteiso* $C_{15:0}$)/$C_{15:0}$

Table 4. Fatty acid concentrations (µg L^{-1}) in spm samples collected at station L4 during the time series 2018 at 25 m.

	01/25	02/18	03/25	04/19	04/30	05/14	05/30	06/25	07/16	08/13	09/17	10/17	11/26	12/10
$C_{12:0}$	0.12	0.01	0.44	0.36	0.07	0.27	0.55	0.74	0.60	0.42	0.36	0.51	0.10	0.29
$C_{14:0}$	1.52	1.31	1.61	2.42	3.05	4.86	9.81	9.03	2.31	3.66	1.51	2.34	1.98	1.37
$BrC_{15:0}$	0.25	0.19	0.25	0.04	0.21	0.34	1.29	0.62	0.52	0.70	0.52	0.66	0.27	0.28
$C_{15:0}$	0.53	0.43	0.57	0.57	0.36	0.65	1.99	0.78	0.67	0.49	0.69	1.18	0.47	0.55
$C_{16:4}$	nd[a]	0.05	nd	nd	0.55	0.50	0.53	0.71	0.38	1.68	0.41	nd	0.42	0.28
$C_{16:1\omega7}$	1.46	1.38	0.86	2.10	3.31	6.67	5.73	8.71	2.50	2.85	2.00	1.65	2.33	1.26
$C_{16:0}$	3.30	3.04	5.10	8.18	3.74	10.32	16.26	10.16	4.24	5.07	3.77	6.27	2.91	3.75
$C_{18:4}$	nd	0.53	0.21	0.75	1.13	1.43	5.19	1.99	0.57	1.45	0.39	0.75	0.97	0.47
$C_{18:1\omega9}$	0.84	0.99	0.49	1.30	1.80	2.23	7.63	3.40	0.82	1.56	1.43	1.53	0.86	0.89
$C_{18:1\omega7}$	0.26	0.27	0.25	0.77	0.39	0.80	1.93	1.11	1.11	1.52	0.74	0.56	0.50	0.35
$C_{18:0}$	1.46	1.57	2.17	3.22	0.20	1.57	2.74	1.18	1.24	0.81	1.61	1.73	0.63	2.52
$C_{20:5}$	nd	1.85	0.16	0.50	3.59	2.69	5.96	3.92	1.19	1.88	1.17	0.81	1.07	0.39
$C_{22:6}$	nd	0.36	nd	nd	2.04	1.21	11.22	2.14	1.26	4.34	1.19	0.92	0.59	0.22
Total fatty acids	9.73	12.00	12.05	20.22	20.46	33.53	71.95	44.69	17.42	27.23	15.81	18.91	13.24	12.69
SFAs (%)	73.7	54.7	83.6	73.2	37.4	53.7	45.4	50.4	55.1	41.0	53.6	67.1	48.0	69.0
MUFAs (%)	26.3	22.0	13.3	20.7	26.9	28.9	21.3	29.6	25.4	21.7	26.4	19.8	27.9	19.7
PUFAs (%)	0	23.3	3.1	6.1	35.7	17.4	33.3	20.0	19.5	37.3	20.0	13.1	24.1	11.3
Diatom fatty acid ratio[b]	0.9	0.9	0.5	0.6	1.9	1.2	1.0	1.8	1.2	1.6	1.0	0.6	1.6	0.8
(MUFAs+PUFAs)/SFAs	0.4	0.8	0.2	0.4	1.7	0.9	1.2	1.0	0.8	1.4	0.9	0.5	1.1	0.5

[a] Not detected

[b] $(C_{14:0} + C_{16:1\omega7} + \Sigma C_{16}$ PUFAs$)/C_{16:0}$

[c] (Σ *iso* and *anteiso* $C_{15:0}$)/$C_{15:0}$

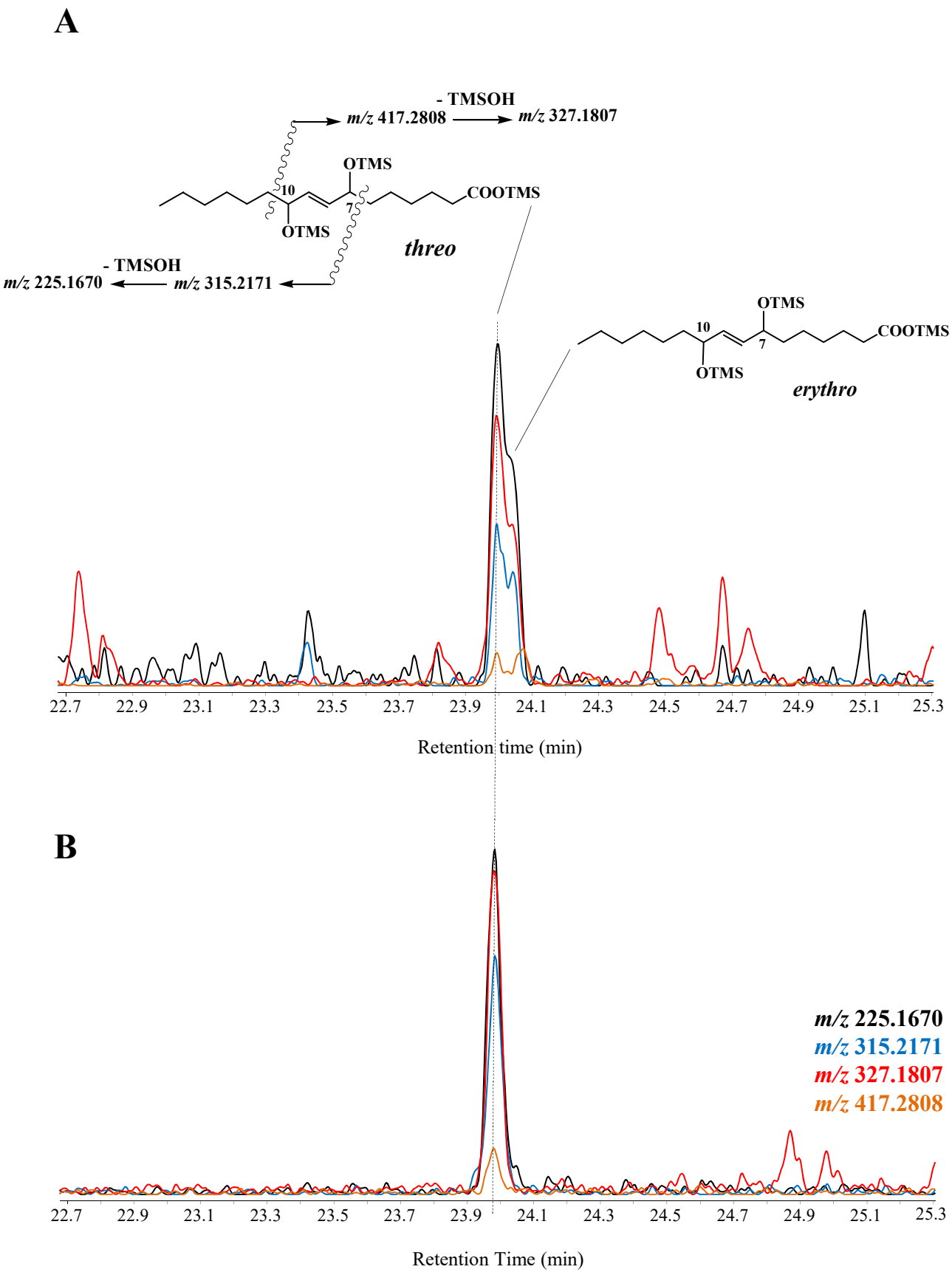
A
- TMSOH
m/z 417.2808
m/z 327.1807
OTMS
10
7
COOTMS
OTMS
threo
- TMSOH
m/z 225.1670
m/z 315.2171
OTMS
10
7
COOTMS
OTMS
erythro
22.7
22.9
23.1
23.3
23.5
23.7
23.9
24.1
24.3
24.5
24.7
24.9
25.1
25.3
Retention time (min)
B
m/z 225.1670
m/z 315.2171
m/z 327.1807
m/z 417.2808
22.7
22.9
23.1
23.3
23.5
23.7
23.9
24.1
24.3
24.5
24.7
24.9
25.1
25.3
Retention Time (min)